Parameter Estimation for Diffusion Models

Torsten Söderström
Susanne Halvarsson

Maj 1999
Uppsala universitet

Rapport 1999-003
ISSN 1404-0603
Institutionen för informationsteknologi

Parameter estimation for diffusion models

T Söderström and S Halvarsson
Department of Systems and Control
Information Technology
Uppsala University

May 25, 1999

Abstract

In many applications, for example in heat diffusion and in flow problems, it is important to describe the process behavior inside the particular medium. An example can be the strive for estimating certain parameters related to the material. This paper describes how the diffusion, modeled by a partial differential equation, can be solved using numerical methods and how results from the field of system identification can be utilized in order to estimate the parameters of interest.

1 Introduction

Diffusion processes are often important in environmental systems. Applications include both diffusion of heat and of pollutions, cf [1, 2, 3]. The diffusion is generally modeled by a partial differential equation (PDE), which may contain some unknown parameters. In order to model such a system these parameters need to be determined.

System identification is a statistical technique for modeling dynamic system [4, 5]. It is then assumed that input-output data are available from an experiment. A model can be fitted to these data using a variety of methods. The dominating effort in system identification has dealt with *black-box* models, in which no a priori information about the system dynamics is used. It is also possible to use *grey-box* models, where physical insight is used to find an appropriately parametrized model [6]. Such models are typically strongly application dependent. So far, it is rather exceptional to fit distributed models by system identification techniques. Some examples in the field include [1, 7, 8, 9]. By 'distributed models' is meant models with a *spatial* distribution, mostly described by means of partial differential equations. In contrast, by 'lumped models' is meant models where the spatial dimension does not appear. Distributed models are relevant for describing phenomena such as

- temperature distribution

- other diffusions
- wave propagation
- flow problems

In physics, the system identification problem is often referred to as an *inverse problem*, that is, given input and output data, determine the underlying system. The *direct problem* is correspondingly in physics defined as the problem of determining the output when the model and the input data are given.

2 A short review of system identification

In what follows, a brief description of model fitting by system identification techniques is given. Consider a dynamic system with input $u(t)$ and output $y(t)$. Assume that discrete time data are available at times $t = h, 2h, \ldots, Nh$, where h is the sampling interval. Further, it is assumed that a linear model of the form

$$y(kh) = G(q;\theta)u(kh) + H(q;\theta)e(kh) \tag{1}$$

is to be fitted to the data. Here q denotes the shift operator ($qu(kh) = \mathrm{u}(kh+h)$, etc), and θ is a vector of the unknown parameters to be determined. In (1), $G(q;\theta)$ and $H(q;\theta)$ are linear filters, and $e(kh)$ denotes a white noise sequence, that is, a sequence of uncorrelated random variables. The purpose of the term $H(q;\theta)e(kh)$ is to account for disturbances such as sensor noise and modeling errors. In black-box models the filters $G(q;\theta)$ and $H(q;\theta)$ are rational, i.e. ratios of polynomials in q. The polynomial coefficients are taken as elements of θ in such a case. The filters $G(q;\theta)$ and $H(q;\theta)$ may have some common parameters.

For the *output error method* (OEM) the noise part of the model is disregarded and θ is determined by minimizing the squared sum of output errors. In case a prefiltering of the data is included and a multi-variable systems is allowed, i.e. systems where u and y are vectors, this generalizes to

$$\hat{\theta} = \arg\min_{\theta} \sum_{k=1}^{N} \parallel L(q)\{y(kh) - G(q;\theta)u(kh)\} \parallel^2 \tag{2}$$

Still a further extension can be to minimize another norm of the output error.

For the *prediction error method* (PEM) the noise properties of the model are taken into account, and the average one step prediction error is minimized. The estimate reads

$$\hat{\theta} = \arg\min_{\theta} \sum_{k=1}^{N} [y(kh) - \hat{y}(kh|kh-h;\theta)]^2 \tag{3}$$

where $\hat{y}(kh|kh-h;\theta)$ is the one-step ahead optimal prediction of the output signal. It turns out that the prediction error for the model (1) can be written as

$$y(kh) - \hat{y}(kh|kh-h;\theta) = H^{-1}(q;\theta)\{y(kh) - G(q;\theta)u(kh)\} \tag{4}$$

There is a rich experience in the literature about various techniques for *model validation*, which concerns assessment whether or not a fitted model reasonably well describes the underlying dynamics. Traditional techniques include various statistical tests, formed from the residuals

$$\varepsilon(kh) = H^{-1}(q;\theta)[y(kh) - G(q;\theta)u(kh)] \tag{5}$$

which for a perfect model should behave as a white noise sequence. As a complement some graphically based approaches can be used for assessing the validity of the model.

In the case when the model parameterization is rich enough to cover the true system dynamics, the parameter estimate $\hat{\theta}$ is, under weak assumptions, consistent, i.e. it converges to the true value, say $\hat{\theta}_o$, as the number of data samples, N, tends to infinity. For large N it can in such cases be said that there is no significant systematic error (i.e. a *bias*) in $\hat{\theta}$. However, there is a stochastic error due to the disturbances. Assuming the true dynamics fulfill

$$y(kh) = G_o(q)u(kh) + H_o(q)e(kh)$$

and that the estimated parameters $\hat{\theta}$ are close to the true ones (hence $G(q;\hat{\theta}) \approx G_o(q)$, $H(q;\hat{\theta}) \approx H_o$). Then the covariance matrix of $\hat{\theta}$ can for large N be approximated as

$$\mathrm{cov}\,(\hat{\theta}) = \frac{\lambda^2}{N}\left[E\left(\frac{d\varepsilon(kh)}{d\theta}\right)^T\left(\frac{d\varepsilon(kh)}{d\theta}\right)\right]^{-1} \tag{6}$$

where $\lambda^2 = Ee^2(kh)$. The standard deviation of $\hat{\theta}$ is thus of magnitude $\lambda/\sqrt{N}$. Note that the covariance expression (6) in general can be estimated from the data.

In the last decade research has been more focused to system identification as a form of *model approximation* or *model reduction*. If the true system dynamics is too complex to be covered by the chosen model parameterization, there will be a systematic error, a bias, in $\hat{\theta}$ even for large data sets. For such cases the prefiltering of the data can have a significant impact on for what frequency range the model fit is good, i.e. for what frequencies ω, $G(e^{i\omega h};\hat{\theta}) \approx G_o(e^{i\omega h})$. In general terms, it is often desirable to choose the model order so that the bias term is not (much) larger than the standard deviation term.

3 A case study: the heat diffusion equation

There are several applications where diffusion models can be used, as described in Section 1. Heat propagation in different media, e.g. solid materials such as

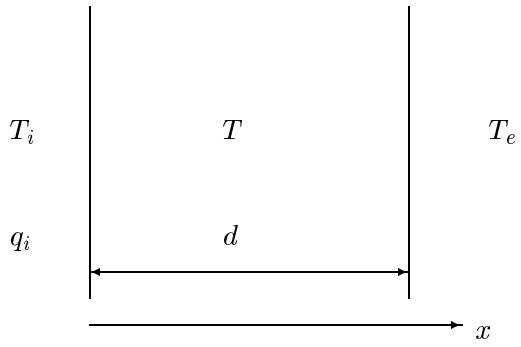

Figure 1: Heat diffusion through a homogeneous wall.

building elements, and liquid media such as water, is of both practical and theoretical interest. It is clear that the heat propagation differs for different media and applications. In this paper, the study is limited to the case of heat diffusion in a homogeneous wall. The main results will be valid for other applications. However, the procedure of taking the Laplace transform of other models of heat propagation and further modeling, might not be obvious.

3.1 Statement of the problem

As an illustrative example, the heat flow through a homogeneous wall of thickness d is examined in some detail. Let x be the coordinate across the wall, T_e the temperature on the exterior side, T_i the temperature on the interior side and q_i the supplied heat on the interior side, cf Figure 1.

Let $T = T(x,t)$ denote the temperature at position x and at time t. Then the heat flow and the temperature are described by

$$\frac{\partial T(x,t)}{\partial t} = \alpha \frac{\partial^2 T(x,t)}{\partial x^2} \tag{7}$$

$$q(x,t) = -\kappa \frac{\partial T(x,t)}{\partial x} \tag{8}$$

where

$$\alpha = \frac{\kappa}{\rho c} \tag{9}$$

Further, κ is the thermal conductivity, ρ the density and c the specific heat capacity.

Consider the wall as a dynamic system with T_e and q_i as input variables and T_i as output. The problem to be considered is thus the following.

Given: Discrete-time data $T_e(h), q_i(h), T_i(h), T_e(2h), q_i(2h), \ldots, T_i(Nh)$.
Find: Parameter estimates of α and κ.

The above problem is apparently an example of grey-box modeling, where physical interpretation has been included in the choice of model.

Needless to say, the geometry in the chosen example is very simple. Nevertheless, the problem is certainly nontrivial, in particular if the data is somewhat corrupted by noise. Note that some of the analysis and identification approaches that will be described are strongly tied to this simple geometry.

Before presenting identification schemes for the stated problem, the model (7), (8) will be examined from a system theoretic perspective.

3.2 The system dynamics

The defined system is linear and has two inputs, q_i and T_e, and one output, T_i. There are several questions that need to be answered before identification of the unknown parameters. What is the system order? How can the state vector be defined? The order is in fact infinite. It is not possible to exactly characterize the dynamics by a finite number of state variables. Instead the whole temperature distribution through the wall, $T(x,t)$, acts as a state vector. This means also that in order to determine the output $T_i(t)$ the initial state $T(x,0)$ needs to be known for all x.

Interestingly enough, one can rather easily derive the transfer function of the system, which will give an input-output description. To do this, first take the Laplace transform of (7) which gives

$$sT(x,s) = \alpha \frac{d^2}{dx^2} T(x,s) \tag{10}$$

where $T(x,s)$ is the Laplace transform of the temperature $T(x,t)$. Regarding s as a fixed parameter, (10) is a standard ordinary differential equation. Then it is found that the general solution to (10) can be written as

$$T(x,s) = F_1(s)\sinh(x\sqrt{\frac{s}{\alpha}}) + F_2(s)\cosh(x\sqrt{\frac{s}{\alpha}}) \tag{11}$$

for some 'constants' $F_1(s)$ and $F_2(s)$. Further, using the Laplace transform on (8) and utilizing (11) gives

$$q(x,s) = -\kappa F_1(s)\sqrt{\frac{s}{\alpha}}\cosh(x\sqrt{\frac{s}{\alpha}}) - \kappa F_2(s)\sqrt{\frac{s}{\alpha}}\sinh(x\sqrt{\frac{s}{\alpha}}) \tag{12}$$

The functions $F_1(s)$ and $F_2(s)$ can be found from the boundary conditions, where (11), (12) have been used

$$\begin{cases} T_i(s) &= T(0,s) = F_2(s) \\ q_i(s) &= q(0,s) = -\kappa F_1(s)\sqrt{\frac{s}{\alpha}} \end{cases} \tag{13}$$

The temperature at the exterior side is thus given by

$$\begin{aligned} T_e(s) &= T(d,s) \\ &= -\frac{q_i(s)}{\kappa\sqrt{s/\alpha}}\sinh\left(d\sqrt{\frac{s}{\alpha}}\right) + T_i(s)\cosh\left(d\sqrt{\frac{s}{\alpha}}\right) \end{aligned} \tag{14}$$

To proceed, introduce some transformed parameters. Set

$$\begin{cases} R \triangleq d/\kappa \ [^oCm^2/W] & \text{thermal resistance} \\ C \triangleq d\rho c \ [Wh/^oCm^2] & \text{thermal capacitance} \\ \tau \triangleq RC \ [h] & \text{time constant} \end{cases} \tag{15}$$

Next note that, using (9), (15)

$$\begin{aligned} d\sqrt{\frac{s}{\alpha}} &= \sqrt{\frac{d^2 s}{\alpha}} = \sqrt{\frac{d^2\rho c}{\kappa}s} = \sqrt{s\tau} \\ \kappa\sqrt{\frac{s}{\alpha}} &= \frac{\kappa}{d}\sqrt{s\tau} = \frac{\sqrt{s\tau}}{R} \end{aligned}$$

Inserting this into (14) gives

$$T_e(s) = -\frac{Rq_i(s)}{\sqrt{s\tau}}\sinh(\sqrt{s\tau}) + T_i(s)\cosh(\sqrt{s\tau})$$

or, rewritten,

$$T_i(s) = \underbrace{R\frac{\tanh(\sqrt{s\tau})}{\sqrt{s\tau}}}_{G_1(s)}q_i(s) + \underbrace{\frac{1}{\cosh(\sqrt{s\tau})}}_{G_2(s)}T_e(s) \tag{16}$$

Equation (16) is a transfer function model that relates q_i and T_e as inputs to T_i as an output. Note that the transfer functions appearing in (16) are transcendental and cannot be written as finite order models. Also note in (16) that $G_1(s)$ and $G_2(s)$ are defined as some functions of $\sqrt{s}$, not of s. However, this is not a contradiction. By series expansion, odd powers of $\sqrt{s}$ will disappear. For example,

$$\cosh(\sqrt{s\tau}) = \sum_{\substack{j=0 \\ j \text{ even}}}^{\infty}\frac{1}{j!}\left(\sqrt{s\tau}\right)^j = \sum_{k=0}^{\infty}\frac{1}{(2k)!}\left(s\tau\right)^k \tag{17}$$

which illustrates that $G_2(s)$ is indeed a function of s rather than of $\sqrt{s}$. It is also worth noticing that $G_1(s)$ and $G_2(s)$ are both of low pass character, see Figure 2. This is an attractive property, as this facilitates approximation with finite order models. (Such an approximation appears inherently during the parameter estimation phase.) Choosing q_i or T_e as the output, i.e. dependent, variable, would though lead to a high pass transfer function.

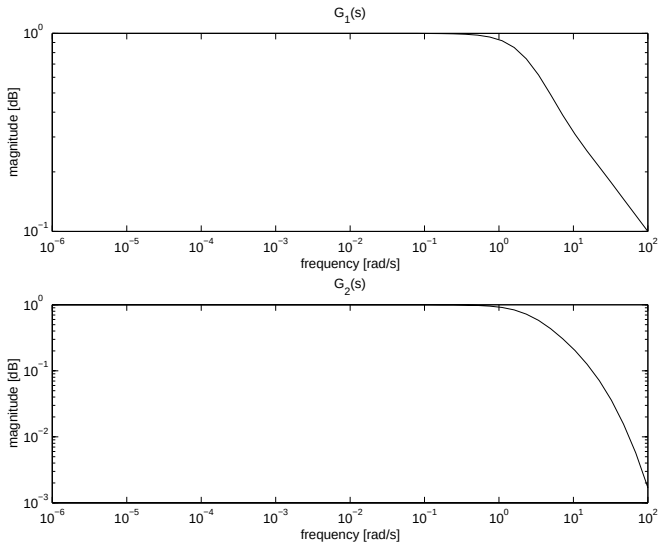

Figure 2: The true transfer functions $G_1(s)$ and $G_2(s)$. The parameters are set to $R = 1$, $C = 1$.

The transfer functions of (16) can also be characterized in terms of poles, zeros and static gain. They have the same set of poles, given by

$$\cosh(\sqrt{s\tau}) = 0 \;\Rightarrow\; e^{\sqrt{s\tau}} + e^{-\sqrt{s\tau}} = 0 \;\Rightarrow\; e^{2\sqrt{s\tau}} = -1 \tag{18}$$

leading to

$$s\tau = -\frac{\pi^2}{4}(2n-1)^2, \qquad n \geq 1 \tag{19}$$

and

$$p_n = -\frac{\pi^2}{\tau}(n - \frac{1}{2})^2, \qquad n = 1, 2, \ldots \tag{20}$$

Only $G_1(s)$ has any zeros. These are given by

$$\sinh(\sqrt{s\tau}) = 0 \qquad (s \neq 0) \;\Rightarrow\; e^{\sqrt{s\tau}} - e^{-\sqrt{s\tau}} = 0 \;\Rightarrow\; e^{2\sqrt{s\tau}} = 1 \tag{21}$$

leading to

$$z_n = -\frac{\pi^2}{\tau}n^2, \qquad n = 1, 2, \ldots \tag{22}$$

Finally, the static gains are

$$G_1(0) = R, \qquad G_2(0) = 1 \tag{23}$$

3.3 Approximate models

There are several ways to approximate the dynamics (7), (8) by a finite order model. Two alternatives will be considered here, namely difference approximation and thermal networks.

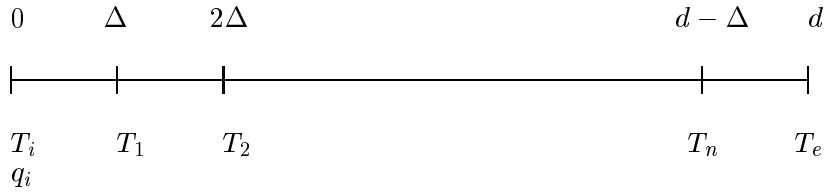

Figure 3: Model of the heat propagation in an homogeneous wall.

3.3.1 Difference approximation

One way to go, that is often used when solving the PDE numerically, is to use a *difference approximation*. Consider approximation of the original model (7), (8) by discretizing the spatial dimension. Divide the wall into $(n+1)$ layers, each of thickness

$$\Delta = \frac{d}{n+1}$$

The temperatures between the different layers can then be used as state variables in a finite order approximate model as shown in Figure 3.

The approximate model reads

$$\begin{cases} \dot{T}_k &= \frac{\alpha}{\Delta^2}(T_{k+1} - 2T_k + T_{k-1}) \qquad k = 1, \dots, n \\ T_o &= T_i, \qquad T_{n+1} = T_e \\ q_i &= -\kappa\frac{1}{\Delta}(T_1 - T_i) \end{cases} \tag{24}$$

Introduce further

$$\beta = \frac{\alpha}{\Delta^2} = \frac{(n+1)^2}{\tau}, \qquad \gamma = \frac{\Delta}{\kappa} = \frac{R}{n+1} \tag{25}$$

Then the approximated model becomes in standard state space form

$$\begin{aligned} \dot{x} &= \beta \begin{pmatrix} -1 & 1 & & 0 & \\ 1 & -2 & 1 & & \\ & & \ddots & & \\ & 0 & & -2 & 1 \\ & & & 1 & -2 \end{pmatrix} x + \beta\gamma \begin{pmatrix} 1 \\ 0 \\ \vdots \\ \\ 0 \end{pmatrix} q_i + \beta \begin{pmatrix} 0 \\ 0 \\ \vdots \\ 0 \\ 1 \end{pmatrix} T_e \\ T_i &= (1 \;\; 0 \;\; \dots \;\; 0)x + \gamma q_i \end{aligned} \tag{26}$$

Rewriting (26) in input-output form gives the approximate transfer functions $\hat{G}_1(s)$ and $\hat{G}_2(s)$. Particularly for model order $n = 2$ the following expressions are obtained.

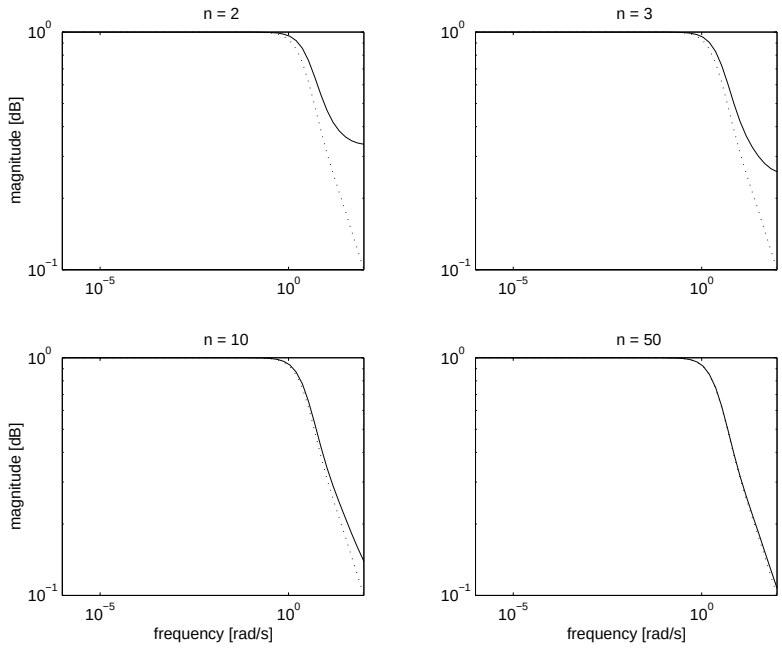

Figure 4: The difference approximation of $G_1(i\omega)$ for some different model orders. The true transfer function (of infinite order) is plotted with a dotted line and the approximate transfer function (of finite order) is plotted with a solid line.

$$\hat{G}_1(s) = \gamma \frac{s^2 + 4\beta s + 3\beta^2}{s^2 + 3\beta s + \beta^2} \qquad \hat{G}_2(s) = \frac{\beta^2}{s^2 + 3\beta s + \beta^2} \tag{27}$$

Figure 4 displays the true transfer function G_1, as given by (16), together with approximations $\hat{G}_1$ for different orders of the difference approximation method. Here, plot (a) shows the case of a second order model and plot (b) shows the result of a third order model. Plots (c) and (d) display the cases of higher order models, $n = 10$ respectively $n = 50$. Figure 5 displays the corresponding for G_2. It can be noted that it might be sufficient to use a rather low order model if the frequencies of interest are low. The deviation of the approximate transfer function from the true transfer function is larger for high frequencies. Also note from Figures 4 and 5 that for a given model order, the approximation of $G_2(s)$ is more accurate than the approximation of $G_1(s)$.

3.3.2 Thermal networks

Another way to approximate the system (7), (8) is to model it as a *thermal network*. This is the thermal equivalence of an electrical RC network. The heat flux corresponds to a current and the temperatures correspond to voltages. As an illustration consider a first order network, see Figure 6.

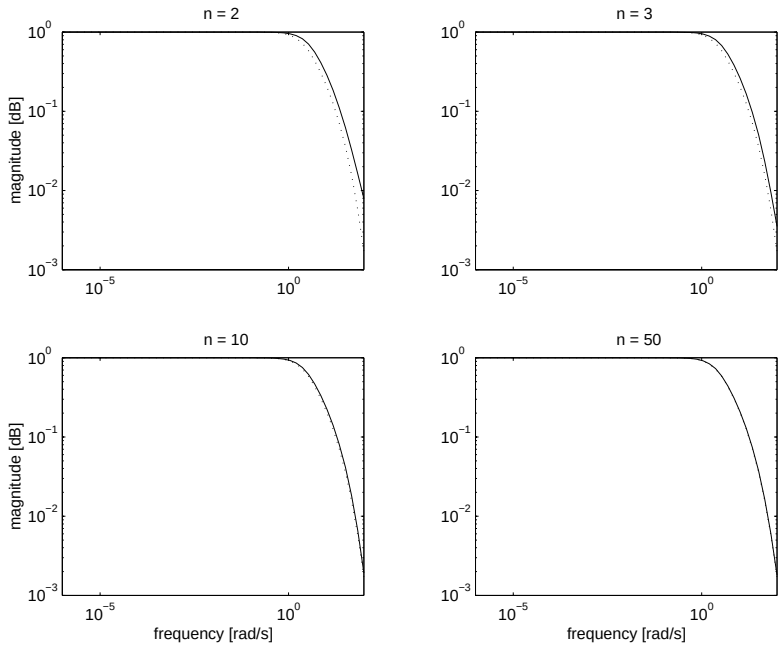

Figure 5: The difference approximation of $G_2(i\omega)$ for some different model orders.

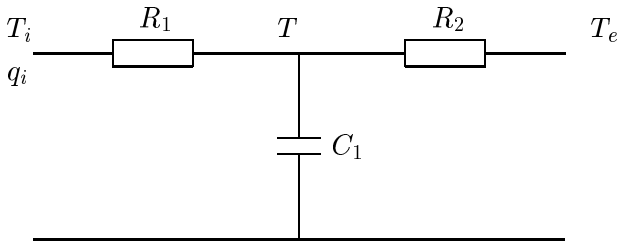

Figure 6: Structure of a first order thermal networks.

For the moment the question of how to choose the parameters R_1, R_2 and C_1 is left for future discussion. To derive the corresponding equations Kirchoff's law is applied.

$$q_i = \frac{T_i - T}{R_1} = \frac{T - T_e}{R_2} + C_1 \frac{dT}{dt} \tag{28}$$

This can be reformulated into a first order model with T as the state, T_e and q_i

as inputs and T_i as output. The result is

$$\begin{cases} \dot{T} &= -\frac{1}{C_1 R_2} T + \frac{1}{C_1} q_i + \frac{1}{C_1 R_2} T_e \\ T_i &= T + R_1 q_i \end{cases} \tag{29}$$

Writing this dynamics in input-output form as

$$T_i(s) = \hat{G}_1(s) q_i(s) + \hat{G}_2(s) T_e(s) \tag{30}$$

results in

$$\hat{G}_1(s) = \frac{R_1 C_1 s + (1 + R_1/R_2)}{C_1(s + 1/C_1 R_2)} \qquad \hat{G}_2(s) = \frac{1}{sC_1 R_2 + 1} \tag{31}$$

One way to choose the network parameters R_1, R_2 and C_1 is to compare $\hat{G}_1(s)$ and $\hat{G}_2(s)$ to the true transfer functions $G_1(s)$ and $G_2(s)$. Require that the static gains as well as the first (dominating) pole and zero coincide. Note that $\hat{G}_2(0) = 1$ automatically. The above idea leads to

$$\frac{1 + R_1/R_2}{1/R_2} = R \tag{32}$$

$$-\frac{1}{C_1 R_2} = -\frac{\pi^2}{4\tau} \tag{33}$$

$$-\frac{1 + R_1/R_2}{R_1 C_1} = -\frac{\pi^2}{\tau} \tag{34}$$

which has the solution

$$R_1 = \frac{R}{4} \qquad R_2 = \frac{3R}{4} \qquad C_1 = \frac{16}{3\pi^2} C \tag{35}$$

A slightly different approach is to require that the approximate model should resemble the true dynamics for low frequencies. Mathematically, this means that the Taylor series expansions of the differences $G_1(s) - \hat{G}_1(s)$ and $G_2(s) - \hat{G}_2(s)$ around $s = 0$ should have no constant terms and zero coefficients for s. Working out the details lead to the equation

$$\begin{aligned} R_1 + R_2 &= R \\ -C_1 R_2^2 &= -\tfrac{1}{3} R\tau \\ -C_1 R_2 &= -\tfrac{1}{2}\tau \end{aligned} \tag{36}$$

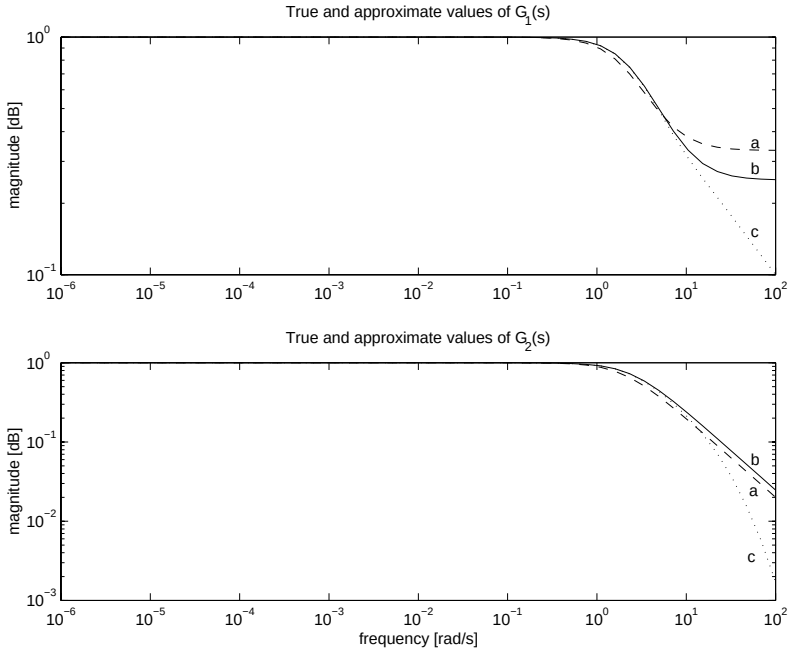

Figure 7: The approximation of $G_1(i\omega)$ and $G_2(i\omega)$ as a thermal network of first order. The upper plot shows approximations of $G_1(s)$. The dashed line (a) shows the approximation obtained from (37) and the solid line (b) the approximation from (35). The true transfer function is drawn with a dotted line (c). The lower plot shows the corresponding for $G_2(s)$. Parameter values used are $R = 1$, $C = 1$.

resulting in the solution

$$R_1 = \frac{1}{3}R \qquad R_2 = \frac{2}{3}R \qquad C_1 = \frac{3}{4}C \tag{37}$$

Note that the parameter values of (35) and (37) differ somewhat.

Figure 7 shows the result of approximation of the transfer functions G_1 and G_2 using a thermal networks of first order. It can be noted that the approximate transfer functions resemble the true ones well for low frequencies. Requiring the same dominating pole, zero and static gain seems to give a slightly better approximation for G_1.

Thermal network models of higher order can also be derived in a similar way, but this paper does not include the details. To indicate the principle, let it suffice to show the structure of a second order thermal network, see Figure 8.

4 Approaches for parameter estimation

In this section a brief presentation of some approaches for the parameter estimation problem introduced in Section 3.1 is given. The next section is devoted

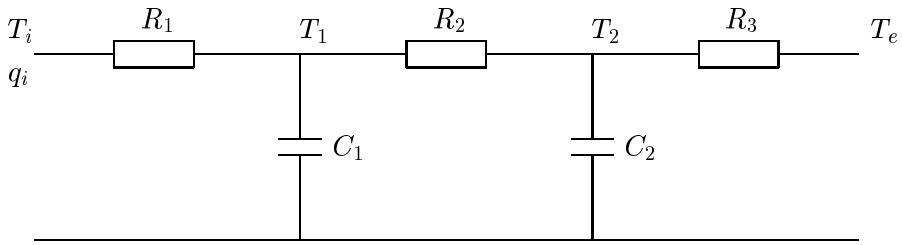

Figure 8: Structure of a second order thermal networks.

to a comparison study using simulated data.

To simplify the notations, and also use some standard symbols, the underlying model will mostly be written as

$$Y(s) = G(s)U(s) \tag{38}$$

where

$$\begin{cases} Y(s) &= T_i(s) \\ G(s) &= [G_1(s) \;\; G_2(s)] \\ U(s) &= [q_i(s) \;\; T_e(s)]^T \end{cases} \tag{39}$$

The quantities $q_i(s)$ and $T_e(s)$ thus act as input signals and $T_i(s)$ as the output. Further let

$$\theta = (R \;\; C)^T \tag{40}$$

denote the parameter vector to be estimated. Of course, the physical parameters α and κ could be introduced as unknowns instead, but these parameters can be derived from (40) using (9) and (15).

4.1 Method 1: A direct approach in the time domain

Let $y^m(kh)$ denote the measured value of the output $y(t)$. Then the following least squares criterion function may be defined

$$V_1(\theta) = \frac{1}{N}\sum_{k=1}^{N}[y^m(kh) - y(kh,\theta)]^2 \tag{41}$$

where $y(t,\theta)$ is the solution to the PDE at time t using the parameter values given by θ, and N is the number of data points available. The estimate $y(t,\theta)$ is obtained either from the infinite order model (16), or from the approximate finite order model (26). These are the approaches normally used to deal with the problem of an infinite order system [8] . The parameter estimate is taken as

$$\hat{\theta}_1 = \arg\min_{\theta} V_1(\theta) \tag{42}$$

This estimate is conceptually simple, but computationally quite complex. As $V_1(\theta)$ depends on θ in a highly nonlinear way, a numerical search procedure is needed to compute $\hat{\theta}_1$. For each function evaluation, the PDE is to be solved for the current value of θ.

The approach can be extended in several ways, for example by

- penalizing another error, e.g. the l^p norm of the error $y^m(kh) - y(kh,\theta)$.
- introducing some prefiltering of the data. As in 'standard system identification', this corresponds to modeling the measurement noise, and to give emphasis to certain frequency bands.

4.2 Method 2: A direct approach in the frequency domain

The idea of this approach is to convert the criterion $V_1(\theta)$ into the frequency domain using Parseval's relation. Let $Y^m(\omega)$ denote the discrete Fourier transform of the time series $\{y^m(kh)\}_{k=1}^N$. Using an FFT algorithm it can conveniently be computed for frequencies $\omega = \frac{2\pi k}{N}$, $k = 0, \ldots, N-1$. Next introduce the criterion

$$\begin{aligned} V_2(\theta) &= \tfrac{1}{K}\textstyle\sum_{j=0}^{K} Q_2\left(j\tfrac{\pi}{Kh}\right)\left|Y^m\left(j\tfrac{\pi}{Kh}\right) - Y\left(j\tfrac{\pi}{Kh},\theta\right)\right|^2 \\ &= \tfrac{1}{K}\textstyle\sum_{j=0}^{K} Q_2\left(j\tfrac{\pi}{Kh}\right)\left|Y^m\left(j\tfrac{\pi}{Kh}\right) - G\left(j\tfrac{\pi}{Kh},\theta\right)U\left(j\tfrac{\pi}{Kh}\right)\right|^2 \end{aligned} \tag{43}$$

where K is the number of frequency points for which the criterion is evaluated. Here, $Q_2(\omega)$ is a user chosen weighting function, with which the deviation $Y^m(\omega) - Y(\omega,\theta)$ can be penalized in different frequency regions. In the particular case study it would be natural to set $Q_2(\omega) \equiv 1$ (no weighting), or to let $Q_2(\omega)$ emphasize the low frequency region, cf the frequency characteristics of the transfer functions in (16).

The parameter estimate for this approach is taken as

$$\hat{\theta}_2 = \arg\min_{\theta} V_2(\theta) \tag{44}$$

There is one potential advantage of this approach over (41), (42). The optimization problem to solve is still nonlinear. However, as the θ-dependence of the function $G(i\omega,\theta)$ is known, the criterion evaluations are much simpler for $V_2(\theta)$ than for $V_1(\theta)$. On the other hand, this approach is limited to linear models for which $G(i\omega,\theta)$ is a known function of the unknown parameter vector θ.

4.3 Methods 3-5: Indirect approaches

The main idea of these approaches is as follows. First the transfer function is estimated by using a standard black-box model of high order, or a smoothed empirical transfer function estimate is used. In any case, by some method an estimated frequency function $\hat{G}(i\omega)$ is available. In the second step a parametric model is fitted to $\hat{G}(i\omega)$.

Ideally the parameter vector θ for which

$$\hat{G}(i\omega) \approx G(i\omega, \theta) \tag{45}$$

is wanted. The dilemma is, of course, that as $\hat{G}(i\omega)$ deviates from the true frequency function, there is no θ that satisfies (45) for all frequencies. There is hence a need to introduce some ways to solve the relation (45) with respect to θ. This can be done in several ways.

- One possibility, that has some similarities to the direct approach in the frequency domain is to choose $\hat{\theta}$ to minimize

$$V_3(\theta) = \frac{1}{K} \sum_{k=0}^{K-1} \left| \hat{G}\left(i\omega(k)\right) - G\left(i\omega(k), \theta\right) \right|^2 Q_3\left(i\omega(k)\right) \tag{46}$$

  where again $Q_3(i\omega(k))$ is a user-defined weighting function, and $\{\omega(k)\}$ are some selected frequency points. In fact this approach may be interpreted as the frequency domain direct approach using a white noise as input. This approach will be regarded as Method 3.

- A second way of treating (45) is to evaluate the two transfer functions in terms of static gain, dominating poles and zeros, and so on. Equating such quantities for $\hat{G}(i\omega)$ and $G(i\omega, \theta)$ leads to a set of equations for determining θ. A further possible quantity to compare is the squared L_2-norm of the transfer functions, $\int_0^\infty |G(i\omega)|^2 d\omega$. In the examples of Section 5, the following criterion is used for this approach,

$$V_4(\theta) = (\hat{G}_1(0) - G_1(0, \theta))^2 + (\hat{p}_1 - p_1)^2 + (\hat{z}_1 - z_1)^2 \tag{47}$$

  where $\hat{G}_1(0)$ is the static gain of the black-box model and $G_1(0, \theta)$ is obtained from (23) using the estimated value of R. The quantities p_1 respective z_1 are the dominating pole and zero from (20) and (22), respectively. Possibly some weighting of the static gain, the dominating pole and the zero can be introduced in (47) in order to emphasize the quantity which is supposed to give the best estimate. In the following, this approach is denoted Method 4.

- A third alternative can be to apply the so called indirect prediction error method, cf [10]. Assume that $\hat{G}(i\omega)$ is obtained from a black-box model, say of order n, with an estimated parameter vector $\hat{\vartheta}$. $\hat{\vartheta}$ is here chosen as the magnitude vector of the estimated transfer function. In practice

a rather good fit to the true transfer function can be expected also for a moderate value of n, as shown in Figures 4 and 5. Next consider a difference approximation (26) of the same order n. When the difference approximation depends only on the parameter vector θ of dimension 2, the parameter vector of the nth order model may in this case be regarded as a mapping $\vartheta(\theta)$. The unknown parameters θ are next determined as the minimization elements of

$$V_5(\theta) = \left(\hat{\vartheta} - \vartheta(\theta)\right)^T Q_5 \left(\hat{\vartheta} - \vartheta(\theta)\right) \tag{48}$$

with Q_5 being a positive definite weighting matrix. The θ dependence of $V_5(\theta)$ can be highly nonlinear and a numerical search is needed. However, if some reasonable initial values are given, a few Gauss Newton iterations for improving the guessed minimum of $V_5(\theta)$ should be sufficient. Finally, this approach is denoted Method 5.

5 Numerical evaluation

5.1 Affecting the bias in the parameter estimates

There are several problems involved in the estimation of material parameters in a distributed system. The first two factors listed below give bias on the parameter estimates. Different realizations of the data also give slightly different biases. Noise, which is mentioned in the third point, gives a variance contribution around the biased mean value of the estimates.

- Firstly, the system is time-continuous, whereas the data are sampled and thus given in time-discrete form. Since sampling has to be performed, some error is introduced. The size of this error depends on the sampling interval.
- Secondly, the continuous system is of infinite order. In order to approximate it using a black-box model, a finite order model must be used. The model order is a user's choice. Different identification methods require different model orders in order to give reliable results. There is a trade-off between having a large model order that can describe the dynamics of the system well, and a low model order that does not give numerical problems and keeps the computational load at a low level. This is a matter of the amount of under-parameterization that can be accepted.
- Thirdly, there is probably some noise, e. g. measurement noise, in the data. Here the study deals with noisy outputs, but in reality even the input data may contain disturbances.

There are some known ways of reducing the influence of the modeling errors that occur caused by the above events. Concerning the first problem, sampling cannot be avoided. However, it is important to try to minimize the effect of it, through careful choice of the sampling interval. It is of importance both to

sample fast enough in order not to loose information about dynamics of the system or signal, and also to use data of sufficient length.

Under-parameterization is not possible to entirely avoid, when a finite order model is used. Therefore, there will inevitable be a systematic error, a bias, on the estimates. The influence of under-parameterization on the estimates can however be reduced by e. g. prefiltering of the data as described in [11]. Also the effect of possible existence of noise on the data can be reduced by prefiltering.

The bias distribution is affected by, [11],

- spectrum of input signal
- prefiltering
- model order
- sampling interval
- noise model
- prediction horizon

That the input spectrum affects the distribution of the modeling error is a known fact in system identification, see (49) – (51). The effect of prefiltering and model order will to some extent be investigated in this paper. The sampling interval is assumed to be short enough not to make the model too coarse. According to [11], there is no disadvantage in using a short sampling interval, except for an increase of the computational load. The measurement noise is assumed to be white Gaussian noise, hence contributing to the measurements $y^m(kh)$ with a constant spectral density over the whole frequency range. For the effect of prediction horizon, see [11].

The output T_i is obtained through the model output, $y^m(kh)$ in (41). Its estimate is obtained from filtering the measured input signals q_i and T_e through estimates of the transfer functions,

$$\hat{T}_i(s) = \hat{G}_1(s)q_i(s) + \hat{G}_2(s)T_e(s) \tag{49}$$

The spectral density of the model output signal is

$$\Phi_{\hat{T}_i}(i\omega) = \left(\hat{G}_1(i\omega)\ \hat{G}_2(i\omega)\right) \begin{pmatrix} \Phi_{q_i}(i\omega) & 0 \\ 0 & \Phi_{T_e}(i\omega) \end{pmatrix} \begin{pmatrix} \hat{G}_1(-i\omega) \\ \hat{G}_2(-i\omega) \end{pmatrix} \tag{50}$$

where Φ denotes spectrum and where q_i and T_e are assumed to be uncorrelated. The error spectrum becomes

$$\Phi_{\tilde{T}_i}(i\omega) = \left(\tilde{G}_1(i\omega)\ \tilde{G}_2(i\omega)\right) \begin{pmatrix} \Phi_{q_i}(i\omega) & 0 \\ 0 & \Phi_{T_e}(i\omega) \end{pmatrix} \begin{pmatrix} \tilde{G}_1(-i\omega) \\ \tilde{G}_2(-i\omega) \end{pmatrix} + \Phi_e(i\omega) \tag{51}$$

where $\tilde{G}_j(i\omega) = G_j(i\omega) - \hat{G}_j(i\omega)$, $j = \{1, 2\}$, and where $\Phi_e(\omega)$ equals the spectrum of possible measurement noise on the output. The error spectrum is

thus dependent on the spectra of the input signal and the measurement noise as well as on the error in the transfer function approximation.

In some cases the user have the opportunity to choose the input signal. In this application, however, the signals are assumed to be given. Prefiltering of the signals was used above to specify for what frequencies the estimated $\hat{G}(s)$ should be a good approximation of the true transfer function. In this case, for example, it is more important to correctly describe the transfer functions for low frequencies up to and including the first pole and zero. It is of importance to have a correct approximation of the static gain and the dominating pole and zero if these specifically are to be used in the identification as is the case for Method 4. The difficulty is then to know where to put the cut-off frequency in the low pass filter, since the dominating pole which specifies the break point in the Bode diagram is not known to the user. (The dominating pole and zero are highly dependent on the unknown material constants R and C). Here it might be possible to use a fairly moderate filter and obtain a rough estimate of the dominating pole and zero, and then perform a new identification with a prefilter adjusted to the obtained approximate model.

When a system is approximated from data, as is done in Section 4.3, the system must be observable. If several modes of the system are badly excited and only weakly observable, it can be hard to make a good approximation of the system. To obtain a good model requires the input data to have energy in the frequency band corresponding to the system, which here is of low-pass character. The input signals thus have to contain energy components in the lower frequency region.

5.2 Choice of input signals

Data are generated and used in order to illustrate the behavior of the different methods for parameter estimation. The signals acting as inputs to the system, T_e and q_i, are chosen to resemble possible outdoor temperature and heat flux, respectively. The data series are of length $N = 16384$ samples and the sampling interval equals $h = 1$ h. Then the system output, T_i, is generated using the continuous-time system (16) in frequency domain with the parameters

$$R = 10\ [^oCm^2/W] \tag{52}$$

$$C = 15\ [Wh/^oCm^2] \tag{53}$$

Finally T_i is transformed back to time domain. The system (16) with the chosen parameter values will thus be considered as the 'true system' in the following.

An example of the signals T_e, T_i and q_i is given in Figure 9. Only parts of the signals are shown. The outdoor temperature is modeled as an AR process with a spectrum corresponding to the daily variations in temperature. The heat flux q_i is modeled in such a way that it somewhat stabilizes the indoor temperature T_i. Figure 10 shows the spectra of the outdoor temperature, T_e, the heat flux,

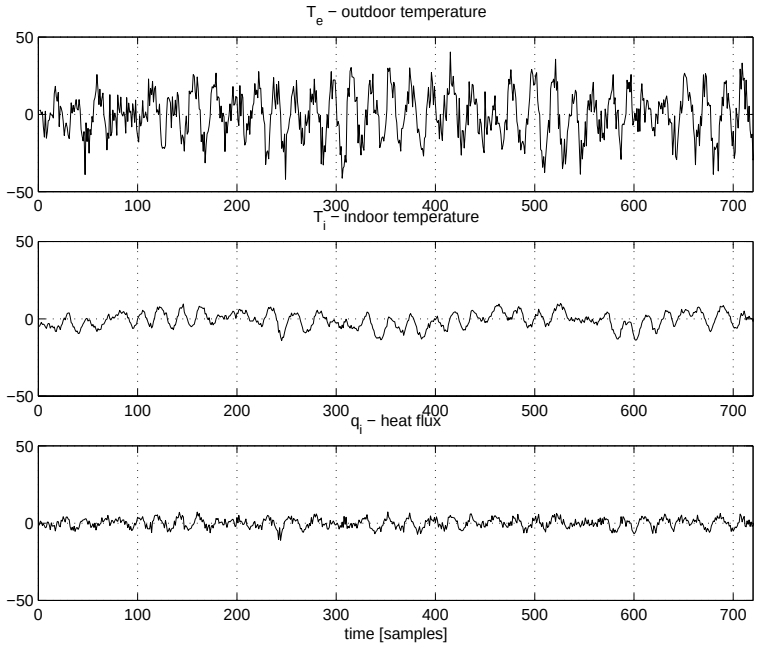

Figure 9: Example of outdoor temperature, indoor temperatures and heat flux.

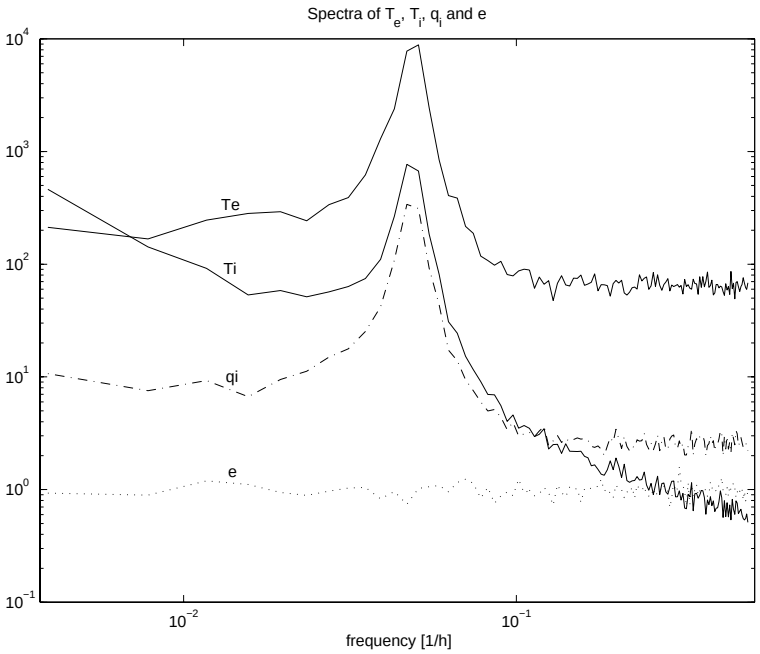

Figure 10: Spectra of temperatures, heat flux and the measurement noise of the indoor temperature. The temperatures are plotted with solid lines.

q_i, the indoor temperature T_i and the measurement noise e, which in some examples is added to the T_i measurements.

Model order n	Computational complexity for Methods 1–5					Comment for Methods 1, 2
	1	2	3	4	5	
∞	440	648				$y(kh, \theta)$ from (16)
10	182	311	36	35	39	$y(kh, \theta)$ from (26)
20	420	668	155	127	169	
30	873	856	352	280	392	
40	2439	1431	624	494	717	

Table 1: Computational complexity for the different methods in Mflops (million floating point operations).

5.3 Computational complexity

The computational load is next considered. The algorithms are implemented in Matlab, and the function *flops* has been used for complexity estimation. The result must be considered with some care, since the implementation may be somewhat 'programmer dependent'. Further, implementation in a digital signal processor (DSP) would give other values of the computational load. Also, different implementations give a variation of the resulting complexity. Rough estimates are determined for each method, and are given in Table 1. The model order n in Table 1 is used in the following ways in the algorithm implementations. For Methods 1, 2 and 5, n equals the model order when the finite order model (26) is used to produce the model output. If the model (16) is used in order to obtain the model output, n is infinite. For Methods 3–5, n determines the order of the ARX-model estimating the transfer function. Note that Method 5 utilizes both (26) and an ARX model in order to approximate the transfer functions in two different ways. The same order n is, however, used.

A comparison of the complexity of the approaches shows that the indirect approaches require less computations than the direct approaches for equal model orders. The difference increases further when taking into account that the direct approaches require larger model orders for similar results, see the simulation results below.

5.4 Sensitivity to parameter variations

It was shown in Section 3.3.1 that the transfer function $G_2(s)$ gives a better approximation for a low model order than $G_1(s)$ does. This can be analytically verified through study of the transfer functions, (16). The transfer function $G_2(i\omega) = 1/\cosh(\sqrt{i\omega\tau})$ is decreasing slowly for ω varying from zero to $1/\tau$ which corresponds to the frequencies of main interest. For $G_1(s)$ on the other

Error in parameter	Affect on $G_1(s)$	Affect on $G_2(s)$
$x\%$ in R	$x\%$ in $G_1(0)$, less for higher freq.	0% in $G_2(0)$, more for higher freq.
$x\%$ in C	0% in $G_1(0)$, more for higher freq.	0% in $G_2(0)$, more for higher freq.
$x\%$ in R *or* C	$\approx x\%$ in dominating pole, zero	
$x\%$ in R *and* C	$\leq 2x\%$ in dominating pole, zero $x\%$ in $G_1(0)$	

Table 2: Effect of modeling errors.

hand, the magnitude depends also on R, which makes the approximation more sensitive to modeling errors. It is also noted that estimation of R and C using only $G_2(s)$ cannot be successful, since $G_2(s)$ depends on the product of the unknown R and C, and not on these parameters individually. A summary of how estimation errors in R and C affect the modeling error of the approximations of $G_1(s)$ and $G_2(s)$ is given in Table 2.

The conclusion of these observations is that it is more difficult to estimate the unknown parameters using $G_2(s)$ when the indirect approaches described in Section 4.3 are considered. In principle, both $G_1(s)$ and $G_2(s)$ could be used at the same time for determination of θ, but here only the approximations of $G_1(s)$ have been used.

5.5 Existence of local minima

When identifying the parameters using a non-linear least squares criterion, the algorithm might get stuck at a local minimum. If this is a risk, an alternative search algorithm, for example an exhaustive search, might be considered. It is thus important to know if the loss function never provides any false minima, i. e. the resulting estimated parameters are always the best possible. However, an example contradicting this utopia is easily produced.

Consider the second transfer function only, $G_2(s) = 1/\cosh(\sqrt{s\tau})$. In the degenerated case, the input signal $T_e(s)$ can be chosen as a sinusoidal. This assumption is not entirely unrealistic, since the temperature (T_e) mainly varies with the day rhythm and thus has a time period of 24 h. The minimization criterion, cf (43), can be written as

$$\begin{aligned} V(\tau) &= E\left[Y^m(s) - Y(s,\tau)\right]^2 \\ &= E\left[\{G_2(s,\tau_0) - G_2(s,\tau)\}U(s)\right]^2 \\ &= E\left[\varepsilon(\tau_0,\tau)\right]^2 \end{aligned} \tag{54}$$

where τ_0 equals the true parameter and τ is the model parameter. Note that $G_2(s)$ depends only on τ and not on the whole parameter vector θ. The following

input signal is used,

$$u(t) = A_u \sin(\omega t) \tag{55}$$

Filtering the input (55) results in a sinusoid with new amplitude and phase. The error function $\varepsilon(\tau_0, \tau)$ can thus be rewritten in the time domain as

$$\begin{aligned} \varepsilon(t, \tau_0, \tau) &= \int \left(g_2(t-v, \tau_0) - g_2(t-v, \tau)\right) u(v) dv \\ &= A_1 \sin(\omega t + \varphi_1) - A_2 \sin(\omega t + \varphi_2) \end{aligned} \tag{56}$$

where $g_2(t, \tau)$ is the weighting function (the inverse Laplace transform of transfer function $G_2(s, \tau)$). In order to determine A_1, A_2, φ_1 and φ_2, rewrite the transfer function $G_2(s)$ as

$$\begin{aligned} G_2(s, \tau_0) &= \frac{1}{\cosh\sqrt{i\omega\tau_0}} \\ &= \frac{1}{\cosh(x_0)\cos(x_0) + i\sinh(x_0)\sin(x_0)} \\ &= \frac{\cosh(x_0)\cos(x_0) - i\sinh(x_0)\sin(x_0)}{(\cosh(x_0)\cos(x_0))^2 + (\sinh(x_0)\sin(x_0))^2} \end{aligned} \tag{57}$$

where

$$x_0 \stackrel{\triangle}{=} \sqrt{\frac{\omega\tau_0}{2}} \tag{58}$$

is used. Similarly, $G_2(s, \tau)$ is expressed using $x \stackrel{\triangle}{=} \sqrt{\omega\tau/2}$. Using (57), the amplitude A_1 now can be expressed as

$$A_1 = A_u |G_2(s, \tau_0)| = A_u \frac{1}{\sqrt{\cosh^2(x_0)\cos^2(x_0) + \sinh^2(x_0)\sin^2(x_0)}} \tag{59}$$

and the phase equals

$$\varphi_1 = -\arctan\left(\frac{\sinh(x_0)\sin(x_0)}{\cosh(x_0)\cos(x_0)}\right) \tag{60}$$

The corresponding holds for A_2 and φ_2 (substitute τ_0 by τ, and x_0 by x). The error function $\varepsilon(t, \tau_0, \tau)$ can now be further developed.

$$\begin{aligned} \varepsilon(t, \tau_0, \tau) &= A_1 \sin(\omega t + \varphi_1) - A_2 \sin(\omega t + \varphi_2) \\ &= (A_1 \cos(\varphi_1) - A_2 \cos(\varphi_2)) \sin(\omega t) \\ &\quad + (A_1 \sin(\varphi_1) - A_2 \sin(\varphi_2)) \cos(\omega t) \\ &\stackrel{\triangle}{=} A_4 \sin(\omega t) + A_5 \cos(\omega t) \\ &= \sqrt{A_4^2 + A_5^2} \sin\left(\omega t + \arctan\left(A_5/A_4\right)\right) \end{aligned} \tag{61}$$

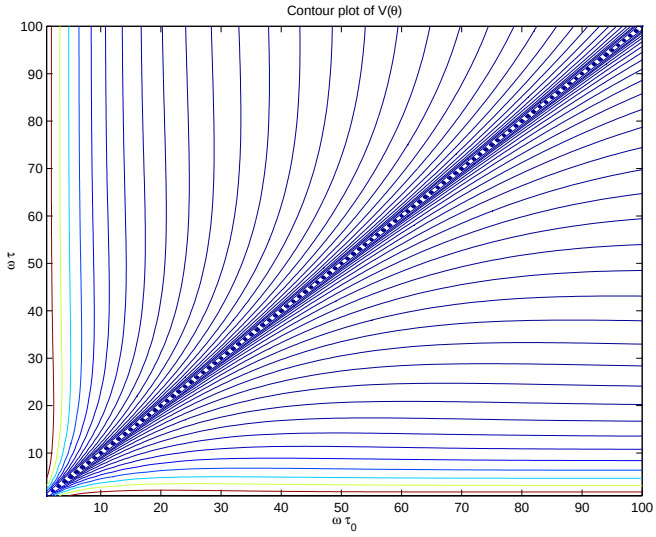

Figure 11: Contour plot of $V(\tau)$ (62).

The criterion (54) can now be expressed as

$$\begin{aligned} V(\tau) &= E\left[\varepsilon(t,\tau_0,\tau)\right]^2 \\ &= \frac{1}{2}(A_4^2 + A_5^2) \\ &= \frac{1}{2}\left(A_1\cos(\varphi_1) - A_2\cos(\varphi_2)\right)^2 + \frac{1}{2}\left(A_1\sin(\varphi_1) - A_2\sin(\varphi_2)\right)^2 \quad (62) \end{aligned}$$

In the following example, $V(\tau)$ is computed for different values of $\omega\tau$ and $\omega\tau_0$. Figure 11 displays the contour plot of $V(\tau)$ for varying $\omega\tau$ and $\omega\tau_0$. The frequency ω should in a real situation equal $\omega = 2\pi f \approx 2\pi/24 \approx 0.26\ [rad/h]$. If the true parameter τ_0 is assumed to be in the interval $\tau_0 \in [6 \quad 150]\ [h]$, then $\omega\tau_0 \in [1.57 \quad 40]\ [rad]$. The exact value of τ_0 depends on the wall element. In order to cover the range of interest, the contour plot is studied in the interval $[1 \quad 100]$. The minima of $V(\tau)$ (corresponding to true and false estimates τ) for different τ_0 where found. With the resolution used in Figure 11, it is not possible to detect any local minima, only the global minimum is clearly visible. For each fixed τ_0, the global minimum appears at $\tau = \tau_0$, as $V(\tau_0) = 0$. A better resolution of Figure 11, however, shows the existence of local minima. Such a result is displayed in Figure 12. The criterion function $V(\tau)$ is computed for values of $\omega\tau$ up to 500. It is clear that several minima exist. The global minimum is always the minimum corresponding to the smallest value of $\omega\tau$. If it is assumed that the input signal, i. e. the outdoor temperature, varies mainly with a 24 h period, values of $\omega\tau$ larger than 40 can be considered as unrealistic. Therefore, only the global, true minimum remains when evaluating the criterion $V(\tau)$, cf Figure 12 in the layer $\omega\tau < 40$. If the usage of a sinusoid as the input signal is considered to be a too rough simplification, the input signal can instead

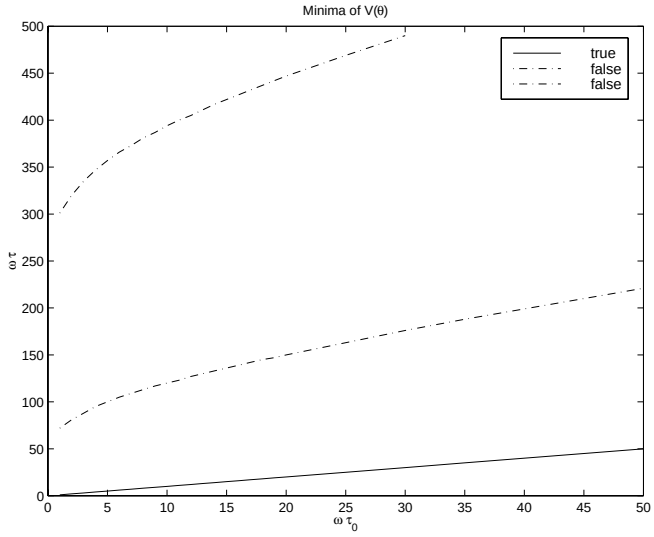

Figure 12: Global and local minima of $V(\tau)$ (62) corresponding to values of $\omega\tau_0 \in [1 \;\; 50]$.

be modeled as a sum of sinusoids,

$$u(t) = \sum_{j=1}^{k} A_{u_j} \sin(\omega t + \varphi_j) \tag{63}$$

The criterion function would then correspondingly be a sum of squared amplitudes

$$V(\tau) = \sum_{j=1}^{k} \frac{A^2(\omega_j)}{2} \tag{64}$$

where the dominating term in (64) corresponds to the main periodicity of the input signal.

In the following, the assumptions made above, that only the second part of the transfer function, $G_2(s)$, is used, and that the input signal is a clean sinusoid, are withdrawn. The input signals are generated according to Section 5.2, and the complete minimization criteria in Section 4 are used in the remaining of this subsection.

In order to determine the possibility of local minima in this case, the shape of the criteria is examined by evaluating them for various values of R and C. If negative parameter values are allowed, it can be shown that several minima exist for some of the criteria. One of the minimum points corresponds to the true solution. Since it is known that the material constants are positive, the minima resulting from one or two negative parameters can be eliminated. The restrictions $R > 0$, $C > 0$ are therefore put on the estimates. Since values of $\tau_0 \in [6 \;\; 150]$ are assumed to be of main interest, R and C varying from 1 to 30

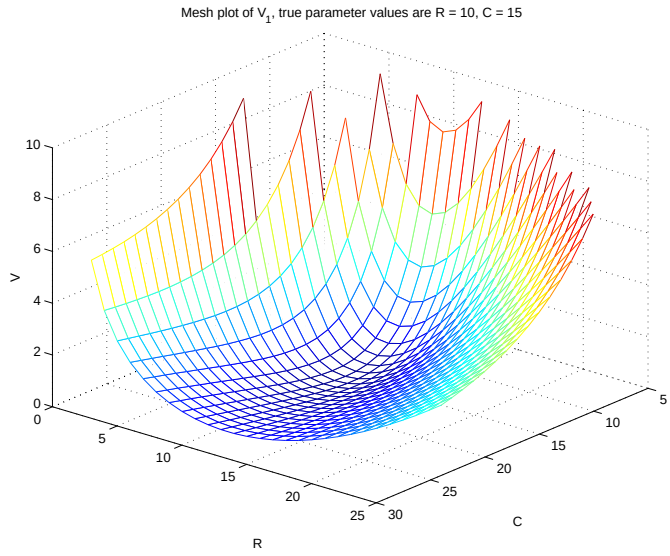

Figure 13: Mesh plot of criterion function V_1, (41), corresponding to Section 4.1. The estimated parameters corresponding to the minimum point are $R = 10$ $[^oCm^2/W$ and $C = 15$ $[Wh/^oCm^2]$ which equals the true values of R and C.

have been used in this study. This restriction was also made in order to limit the computational load.

As examples, the criteria (41) and (46) are plotted for different integer values of R and C in the estimated model. The model order was here chosen as $n = 50$ and no noise was applied to any of the signals. Results are shown in Figures 13 – 15. Note that the restriction of using integer values of R and C of course not is used when estimating the parameters R and C in Section 5.7.

Criterion for direct approach in the time domain
In Figure 13 the criterion V_1 (41) for the direct time domain approach in Section 4.1 is shown. Criterion values above 10 are ignored in the plot, in order to show the shape of the function. The criterion function has a smooth surface leaning towards the minimum point, which corresponds to the true parameter values.

Criterion for indirect approach in the frequency domain
Figure 14 shows the criterion V_3 associated with the transfer function $G_1(s)$ for positive values of θ only. The minimum is at $R = 10$ $[^oCm^2/W]$, $C = 15$ $[Wh/^oCm^2]$, which are also the true parameter values. Criterion values above 9 are ignored in the plot.

Figure 15 displays the criterion V_3 associated with the transfer function $G_2(s)$, where $Q_3 \equiv 1$. Several global minima exist for different positive values of R and C. In fact, a minimum is found whenever $\hat{R}\hat{C} \approx RC$. Some minima corresponding to integer values of $\hat{R}$ and $\hat{C}$ are marked by circles in the figure. The fact that there are more than one minimum, is also obvious from the second

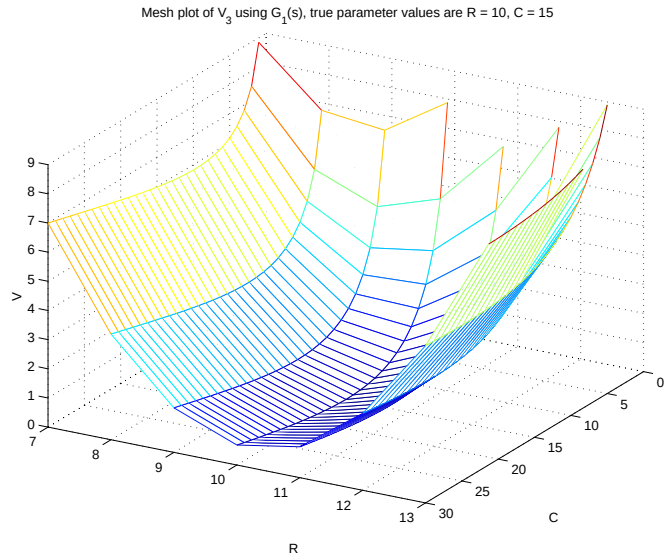

Figure 14: Mesh plot of criterion function V_3, (46), using $G_1(i\omega)$ corresponding to Section 4.3. The plot shows the criterion function around minimum only.

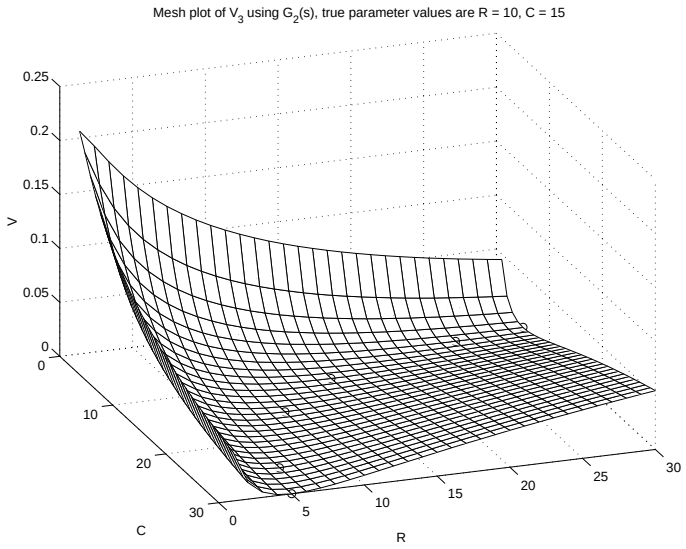

Figure 15: Mesh plot of criterion function V_3 using $G_2(i\omega)$ corresponding to Section 4.3. The minimum points are indicated by circles in the figure.

part of (16). The same estimated transfer function results for different values of the parameters, since only the product $RC = \tau$ affects $G_2(s)$.

As a conclusion, analyzing the criteria (41), (43), (46), (47) and (48) for some values of the parameters, shows that the criteria are well-behaved if only positive parameters are considered. The minimum is then given, as expected, close to the true parameters in the examples. The deviation is small and due to the approximation introduced by using $n < \infty$. For the indirect approaches unique-

ness problems occur if only $G_2(s)$ is used. This is natural as $G_2(s)$ depends only on one parameter, namely τ, and not on R, see (16).

5.6 Model validation

If $y(t,\theta)$ is obtained from the approximate finite order model (26), some numerical errors are introduced due to the discretization in space. The difference between the approximated temperature T_k and the exact temperature in each point k converges as $O(\Delta^2)$, [12], i. e. the introduced error decreases quadratically as the number of layers increases. One way to estimate the error more accurately, is to use Richardson extrapolation [12], i. e. derive the model for two different model orders, e. g. n and $2n$, using (26). After conversion to discrete time, which is assumed to introduce neglectable errors compared to the errors due to finite order models, $y(n,kh)$ and $y(2n,kh)$ result. The model outputs can then, according to the statement above, be approximated as

$$y(n,kh) \approx y(kh) + \frac{C(kh)}{n^2} \tag{65}$$

$$y(2n,kh) \approx y(kh) + \frac{C(kh)}{4n^2} \tag{66}$$

where $y(kh)$ is an improved approximation of the PDE and $\{C(kh)\}$, $k = 1,2,\ldots,N$, is a vector of proportional constants. Comparing the results of (65) and (66), $C(kh)$ and $y(kh)$ are computed as

$$C(kh) \approx \frac{4n^2}{3}\left(y(n,kh) - y(2n,kh)\right) \tag{67}$$

$$y(kh) \approx \frac{4}{3}y(2n,kh) - \frac{1}{3}y(n,kh) \tag{68}$$

The relative error may be defined as

$$R(n) = \frac{\sqrt{\sum_{k=1}^{N}\frac{C^2(kh)}{n^4}}}{\sqrt{\sum_{k=1}^{N}y^2(kh)}} \approx \frac{\sqrt{\sum_{k=1}^{N}\frac{C^2(kh)}{n^4}}}{\sqrt{\sum_{k=1}^{N}\left(y(n,kh) - \frac{C(kh)}{n^2}\right)^2}} \tag{69}$$

Inserting the expression of $C(kh)$ from (67) gives the relative error as function of model outputs,

$$R(n) = 4\frac{\sqrt{\sum_{k=1}^{N}\left(y(n,kh) - y(2n,kh)\right)^2}}{\sqrt{\sum_{k=1}^{N}\left(4y(2n,kh) - y(n,kh)\right)^2}} \tag{70}$$

The *approximate* model order required to obtain a certain error can be determined from $R(n)$, see Figure 16, which shows the relative error $R(n)$ as a function of the model order n. Here the simulation is made using one realization of the data with $\theta^T = [10\ 15]$, generated according to Section 5.2. The relative error is determined from the second part of (69), where $C(kh)$ is obtained from

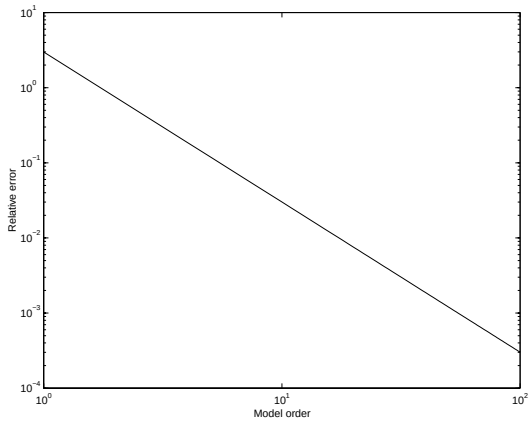

Figure 16: Relative error $R(n)$, (69), due to the use of finite order model.

(67) using $n = 10$. In order to obtain a relative error of for example 1 %, a model order larger than 17 must be chosen for the particular data realization used here. Other realizations give, of course, slightly different values of $R(n)$.

It would be useful to have methods to determine an appropriate model order, using available data. The resulting 'best' model order differs depending on which estimation method that is used. It is extra important to determine a good model order when there is a risk for numerical problems when a too high model order is used. One way to determine the appropriate model order is to utilize the Akaike's information criterion (AIC). The AIC criterion is defined as

$$\text{AIC} = N \log V(n) + 2p \tag{71}$$

where $V(n)$ is the minimal value of the loss function for model order n. The quantity p equals the number of unknown parameters in the scheme, which is $p = 2n$ when an ARX model of order n is fitted. The following scheme is used.

Scheme for model validation

1. Choose a maximum model order $NMAX$
2. Choose model order $n = 1$.
3. Determine the AIC (71) for the specific model order n.
4. If warnings are given that the condition number when solving the normal equation is too large, go to Step 6.
5. Set $n = n + 1$. If $n \leq NMAX$, and go to Step 3, else go to Step 6.
6. Choose the model order n which gives the smallest AIC value, but does not give numerical problems.

This test has been performed for Method 3 where it is important not to choose a too large model order which would result in numerical problems. The loss function $V(n)$ in the AIC criterion is in this study chosen to be implemented as

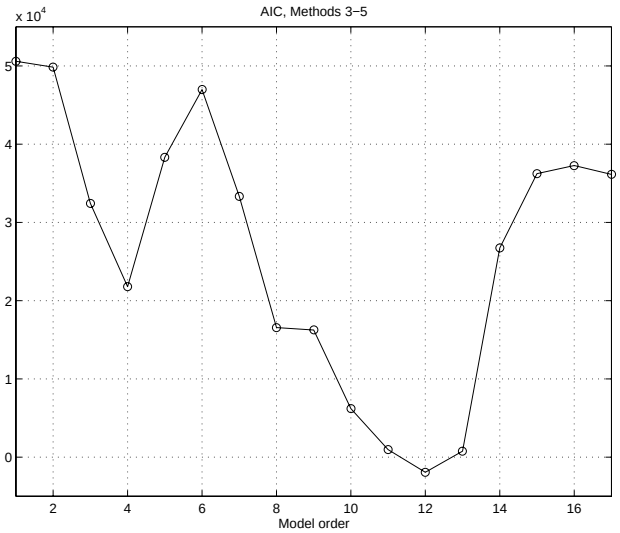

Figure 17: AIC for determination of model order for Methods 3-5.

(cf (46))

$$V(n) = \sum_{k=0}^{K-1} [\hat{G}_1(n, i\omega(k)) - G_1(i\omega(k), \hat{\theta})]^2 \tag{72}$$

where $\hat{G}_1(n, i\omega)$ originates from the black-box model approximation of order n. The estimate $G_1(i\omega, \hat{\theta})$ comes from the first part of the infinite order model (16) using approximated parameters $\hat{R}$ and $\hat{C}$. The parameter vector $\hat{\theta} = (\hat{R}\ \hat{C})^T$ was determined by minimization of (46) for model order n, and ω is a sequence of selected frequency points. Figure 17 shows the resulting AIC values for different model orders up to order 17, where the first warning about numerical problems occurred. Model order $n = 12$ gives the smallest AIC value, which then is the best model order according to the scheme above. For larger model orders it can be seen that the criterion (71) increases, probably due to large condition number of the normal equation, leaving too few bits for a good numerical precision in the calculations. Note also a local minimum occurs for $n = 4$!

The model validation scheme was also applied on Methods 1–2. Here, there is no risk for numerical problems due to large model orders. The AIC criterion is implemented using the loss function

$$V(n) = \frac{1}{N} \sum_{k=1}^{N} [y^m(kh) - y(kh, \theta)]^2 \tag{73}$$

where $y^m(kh)$ is the measured system output and where $y(kh, \theta)$ is the model output. Figure 18 shows the resulting AIC values for Method 1 for model orders varying from 2 to 54. Only values for every fourth order are computed. It is not surprisingly that the AIC decreases for increasing model orders. Since dim $\theta = 2$, it is not likely that the Hessian V'' becomes badly conditioned, even

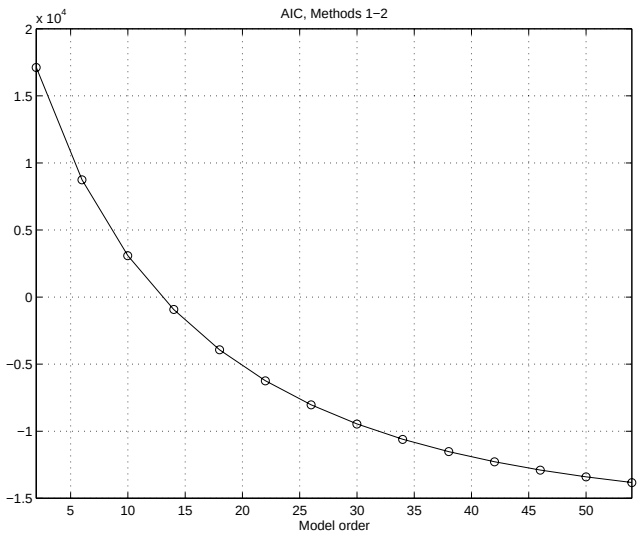

Figure 18: AIC for determination of model order for Methods 1-2.

	Noise free data	Noisy data
No prefiltering	Section 5.7.1	Section 5.7.2
Prefiltering	Section 5.7.1	Section 5.7.2

Table 3: The different cases treated.

for large n. There is thus no reason to expect any numerical problems for the direct methods. The result indicates that as n grows, the model output $y(kh, \theta)$ will resemble the system output $y^m(kh)$ better and better. The computational load increases of course accordingly, cf Section 5.3.

5.7 Results of numerical evaluation

The estimation methods are tested using data generated according to Section 5.2 under various conditions, namely with and without noise on the output and with and without prefiltering of the signals. A summary of the different cases are given in Table 3 together with the section numbers in which they are treated.

Simulations have been performed using ten different realizations of the data. For each realization, both a noise free and a noise corrupted output have been considered. Thus, 20 different signal sets have been used, where the same noise free data have been used in every two sets, one of which was corrupted by noise on the output. This means that comparison between the cases can be made without concern that the input signals have been different. An average of the resulting parameter estimates is given in the tables. When an approximate transfer function has been computed (indirect approaches), logarithmic distributed frequencies have been considered in the interval $\omega \in [10^{-6}, 1]$, where the frequency band is supposed to cover frequencies from a value close to zero to frequencies well above $1/\tau$. In the examples $\tau = RC$ equals 150 [h], giving

$1/\tau = 0.0067[h^{-1}]$.

For a few data realizations and model orders, the algorithms give quite bad estimates. This can typically happen for Methods 3-5, where a large model order may give rise to bad numerical accuracy due to a large condition number of the normal equation. A scheme for evaluation of parameter estimates is implemented in order to detect such situations. If the scheme indicates that for a particular data set, the estimate of the frequency function $\hat{G}(i\omega)$ is not reliable, that particularly realization is not used in the final result presented in the tables in the following sections. It is indicated in the tables if there are any rejected realizations.

Scheme for evaluation of parameter estimates

1. Estimate the parameters R and C using the whole data series of length N, resulting in $\hat{R}$, $\hat{C}$.
2. Estimate the parameters R and C using the first half of the data series, i. e. $1 : N/2$, resulting in $\hat{R}_1$, $\hat{C}_1$.
3. Estimate the parameters R and C using the second half of the data series, i. e. $N/2 + 1 : N$, resulting in $\hat{R}_2$, $\hat{C}_2$.
4. Since a long data series is used in the simulations, steps 2 and 3 should give similar results. Therefore a simple comparison of the resulting estimates gives an indication of the reliability and accuracy of the estimates. Compute

$$\Delta_R = \frac{\hat{R} - \hat{R}_1}{\hat{R}} + \frac{\hat{R} - \hat{R}_2}{\hat{R}} \tag{74}$$

$$\Delta_C = \frac{\hat{C} - \hat{C}_1}{\hat{C}} + \frac{\hat{C} - \hat{C}_2}{\hat{C}} \tag{75}$$

   The result of the data realization is rejected if either $|\Delta_R| > 0.1$ or $|\Delta_C| > 0.1$, which corresponds to an allowed discrepancy of 10 %.

5.7.1 Identification from noise free data

Results of the different estimation approaches for various model orders are summarized in Tables 4–7. In Tables 5, 7, 10 and 12, model orders up to 12 only are used. This is due to the numerical problems that can occur for higher model orders for Methods 3–5. The model (26) used in Methods 1–2 does not give rise to such numerical problems.

As can be seen, a bias appears in many of the estimates. Since no noise is present here, the estimation error is due to an imperfect approximation of the transfer functions, cf Section 4. There are two important aspects to consider when approximating the transfer functions.

Model order n	Results from Methods 1–2 1	2	Rejections 1	2
10	$\hat{R} = 7.80$	$\hat{R} = 9.72$	–	–
	$\hat{C} = 17.81$	$\hat{C} = 23.70$	–	–
15	$\hat{R} = 8.62$	$\hat{R} = 10.10$	–	–
	$\hat{C} = 17.01$	$\hat{C} = 20.68$	–	–
20	$\hat{R} = 9.04$	$\hat{R} = 10.07$	–	–
	$\hat{C} = 16.57$	$\hat{C} = 18.85$	–	–
30	$\hat{R} = 9.44$	$\hat{R} = 10.00$	–	–
	$\hat{C} = 16.08$	$\hat{C} = 17.21$	–	–
40	$\hat{R} = 9.62$	$\hat{R} = 9.95$	–	–
	$\hat{C} = 15.80$	$\hat{C} = 16.48$	–	–
50	$\hat{R} = 9.71$	$\hat{R} = 10.00$	–	–
	$\hat{C} = 15.62$	$\hat{C} = 17.21$	–	–
∞	$\hat{R} = 10.00$	$\hat{R} = 10.00$	–	–
	$\hat{C} = 15.00$	$\hat{C} = 15.00$	–	–

Table 4: Result of parameter estimation, Methods 1–2, no noise, no prefiltering of the signals. In the true system, R equals 10 $[^oCm^2/W]$ and C equals 15 $[Wh/^oCm^2]$. The column *Rejections* indicates how many realizations that were rejected for each method.

i. A small model order n cannot describe the system dynamics correctly and results in bad parameter estimates.

ii. For the black-box model used in Methods 3–5, a large model order often leads to numerical problems which in turn may give bad estimations.

The true transfer functions of infinite order are approximated using the difference approximation method in Methods 1, 2 and 5, and using an ARX model of finite order in Methods 3 – 5. Since finite order models are used, bias in the transfer function estimates cannot be avoided. Exceptions are Method 1 and 2 for the case when infinite order models (16) are used, cf Table 4.

For Method 3, the whole transfer function estimate is used in the criterion. This gives, compared to Method 4 where only three points in the transfer function are used, some drawbacks:

i. The estimated transfer function must be fitted for all frequencies, also higher frequencies for which it is more difficult to estimate it correctly.

ii. The whole transfer function approximated using the ARX model must be converted to continuous time in order to build the criterion. For Method 4, only three points in the frequency function need to be transformed.

Model order	Results from Methods 3–5			Rejections		
n	3	4	5	3	4	5
4	$\hat{R} = 10.39$	$\hat{R} = 10.38$	$\hat{R} = 10.36$	–	–	–
	$\hat{C} = 10.47$	$\hat{C} = 5.08$	$\hat{C} = 14.39$	–	–	–
6	$\hat{R} = 15.86$	$\hat{R} = 15.86$	$\hat{R} = 15.84$	–	–	–
	$\hat{C} = 23.33$	$\hat{C} = 18.47$	$\hat{C} = 29.56$	–	–	–
8	$\hat{R} = 9.59$	$\hat{R} = 9.57$	$\hat{R} = 9.59$	–	–	–
	$\hat{C} = 10.36$	$\hat{C} = 1.99$	$\hat{C} = 12.29$	–	–	–
10	$\hat{R} = 10.30$	$\hat{R} = 10.30$	$\hat{R} = 10.30$	–	–	–
	$\hat{C} = 15.13$	$\hat{C} = 14.84$	$\hat{C} = 17.56$	–	–	–
11	$\hat{R} = 10.16$	$\hat{R} = 10.30$	$\hat{R} = 10.30$	–	–	–
	$\hat{C} = 14.88$	$\hat{C} = 14.84$	$\hat{C} = 17.56$	–	–	–
12	$\hat{R} = 10.01$	$\hat{R} = 10.01$	$\hat{R} = 10.02$	–	–	–
	$\hat{C} = 14.71$	$\hat{C} = 14.86$	$\hat{C} = 16.67$	–	–	–

Table 5: Result of parameter estimation, Methods 3–5, no noise, no prefiltering of the signals. In the true system, R equals 10 $[^oCm^2/W]$ and C equals 15 $[Wh/^oCm^2]$.

These points correspond to the dominating pole, the dominating zero and the static gain.

In Tables 6–7 the result is displayed for the noise free case, but when the data was prefiltered through a low pass filter. The filter is implemented as a second order Butterworth filter with a cut-off frequency of 1/(12h).

Comparing the results presented in Tables 4, 5 and 6, 7, it is obvious that a better estimate can be gained by prefiltering of the data. Note also that the estimated parameters remain unbiased if the infinite order model is used (Methods 1–2).

In Figures 19 and 20, the bias and standard deviation of estimates of Method 1 and 3 are presented, as a complement to the tables.

It can be noted that $\hat{R}$ is more accurate than $\hat{C}$ for equal model orders. The fact that it is easier to estimate R than C can be theoretically verified by considering the second derivative of the loss function. The bias, as well as the covariance, of the estimates are dependent of the inverse of the Hessian, $(V'')^{-1}$, [4]. Therefore, $(V'')^{-1}$ gives a good indication of the variance of $\hat{R}$ and $\hat{C}$. For determination of $\hat{\theta}$, it is important that $(V'')^{-1}$ is nonsingular. The requirement of non-singularity holds under quite general conditions when the system is in the model set. For underparametrized models, as in this case, the condition number gives important information about the solution uncertainty. If the condition number of the Hessian is small, the Hessian is said to be well

Model order n	Results from Methods 1–2 1	2	Rejections 1	2
10	$\hat{R} = 8.64$	$\hat{R} = 9.42$	–	–
	$\hat{C} = 18.05$	$\hat{C} = 18.93$	–	–
15	$\hat{R} = 9.18$	$\hat{R} = 9.70$	–	1
	$\hat{C} = 17.10$	$\hat{C} = 17.63$	–	–
20	$\hat{R} = 9.42$	$\hat{R} = 9.72$	–	1
	$\hat{C} = 16.59$	$\hat{C} = 16.81$	–	–
30	$\hat{R} = 9.65$	$\hat{R} = 9.83$	–	1
	$\hat{C} = 16.06$	$\hat{C} = 16.16$	–	–
40	$\hat{R} = 9.75$	$\hat{R} = 9.83$	–	–
	$\hat{C} = 15.78$	$\hat{C} = 15.75$	–	–
50	$\hat{R} = 9.80$	$\hat{R} = 9.83$	–	–
	$\hat{C} = 15.61$	$\hat{C} = 16.16$	–	–
∞	$\hat{R} = 10.00$	$\hat{R} = 10.00$	–	–
	$\hat{C} = 15.00$	$\hat{C} = 15.00$	–	–

Table 6: Result of parameter estimation in the noise free case, Methods 1–2. The data are filtered through a low pass filter. In the true system, R equals 10 $[^oCm^2/W]$ and C equals 15 $[Wh/^oCm^2]$. The column *Rejections* indicates how many realizations that were rejected for each method.

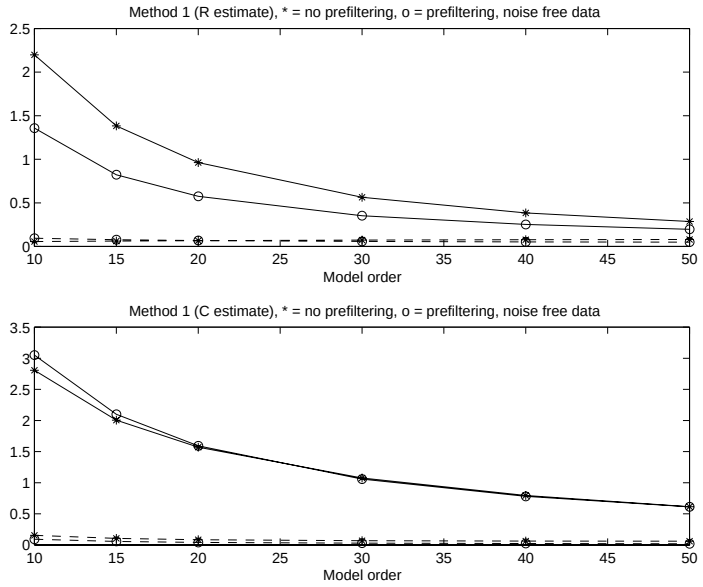

Figure 19: Bias (solid lines) and standard deviation (dashed lines) of $\hat{R}$ and $\hat{C}$ obtained from Method 1 in the noise free case. Lines with stars ($*$) indicate no prefiltering and circles (o) indicate prefiltering of data.

Model order	Results from Methods 3–5			Rejections		
n	3	4	5	3	4	5
4	$\hat{R} = 11.00$	$\hat{R} = 11.02$	$\hat{R} = 10.98$	–	–	–
	$\hat{C} = 17.61$	$\hat{C} = 28.38$	$\hat{C} = 24.95$	–	–	–
6	$\hat{R} = 10.00$	$\hat{R} = 10.00$	$\hat{R} = 10.00$	–	–	–
	$\hat{C} = 14.18$	$\hat{C} = 12.37$	$\hat{C} = 17.95$	–	–	–
8	$\hat{R} = 10.34$	$\hat{R} = 10.34$	$\hat{R} = 10.34$	–	–	–
	$\hat{C} = 15.09$	$\hat{C} = 14.79$	$\hat{C} = 18.13$	–	–	–
10	$\hat{R} = 10.13$	$\hat{R} = 10.10$	$\hat{R} = 10.14$ –	–	2	
	$\hat{C} = 14.81$	$\hat{C} = 15.61$	$\hat{C} = 17.18$	–	–	–
11	$\hat{R} = 10.44$	$\hat{R} = 10.11$	$\hat{R} = 10.15$	1	3	1
	$\hat{C} = 15.40$	$\hat{C} = 15.67$	$\hat{C} = 17.17$	–	–	
12	$\hat{R} = 10.10$	$\hat{R} = 10.09$	$\hat{R} = 10.11$	3	5	3
	$\hat{C} = 14.82$	$\hat{C} = 13.87$	$\hat{C} = 16.78$	–	–	

Table 7: Result of parameter estimation in the noise free case, Methods 3–5. The data are filtered through a low pass filter. In the true system, R equals 10 $[^oCm^2/W]$ and C equals 15 $[Wh/^oCm^2]$.

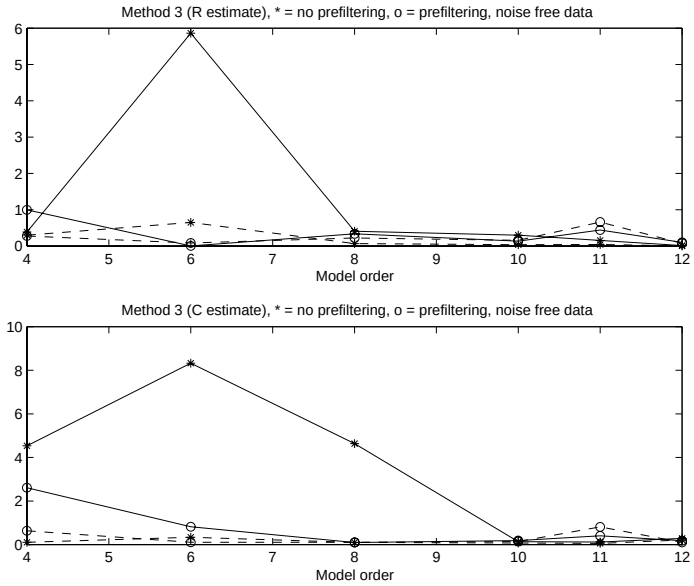

Figure 20: Bias (solid lines) and standard deviation (dashed lines) of $\hat{R}$ and $\hat{C}$ obtained from Method 3 in the noise free case. Lines with stars ($*$) indicate no prefiltering and circles (o) indicate prefiltering of data. With prefiltering, data realizations were rejected once for $n = 11$ and three times for $n = 12$ (out of ten).

conditioned. If the condition number is large, the Hessian is badly conditioned, and the relative uncertainty of the solution is large. This means that a small perturbation of the data can give a large error in the solution, which of course in undesirable.

The Hessian,

$$V'' = \begin{pmatrix} \frac{\partial^2 V}{\partial R^2} & \frac{\partial^2 V}{\partial R \partial C} \\ \frac{\partial^2 V}{\partial C \partial R} & \frac{\partial^2 V}{\partial C^2} \end{pmatrix} \tag{76}$$

can be approximated as

$$\begin{cases} \frac{\partial^2 V}{\partial R^2} & \approx & \frac{1}{(\Delta R)^2}\left[V(R-\Delta R, C) - 2V(R,C) + V(R+\Delta R, C)\right] \\ \frac{\partial^2 V}{\partial C^2} & \approx & \frac{1}{(\Delta C)^2}\left[V(R, C-\Delta C) - 2V(R,C) + V(R, C+\Delta C)\right] \\ \frac{\partial^2 V}{\partial R \partial C} & \approx & \frac{1}{4\Delta R \Delta C}\left[V(R+\Delta R, C+\Delta C) - V(R+\Delta R, C-\Delta C)\right. \\ & & \left. -V(R-\Delta R, C+\Delta C) + V(R-\Delta R, C-\Delta C)\right] \end{cases} \tag{77}$$

where $\frac{\partial^2 V}{\partial R \partial C} = \frac{\partial^2 V}{\partial C \partial R}$ and ΔR and ΔC are small changes in the R and C directions, respectively. The derivatives in (77) are derived using a central difference quotient in R and C, respectively. After series expansion, the approximation (77) can be shown to give the error

$$\mathrm{err}(V'') = \begin{pmatrix} O(\Delta R^2) & O\left(\frac{\Delta R^2}{\Delta C}\right) + O\left(\frac{\Delta C^2}{\Delta R}\right) \\ O\left(\frac{\Delta R^2}{\Delta C}\right) + O\left(\frac{\Delta C^2}{\Delta R}\right) & O(\Delta C^2) \end{pmatrix} \tag{78}$$

Choosing e.g. $\Delta R = \Delta C = 0.1$ gives for one particular realization of the data for the different methods the second derivative according to Table 8. Also, the condition numbers of V'' for the methods are displayed. For Methods 1–2, model order 50 was used, and for Methods 3–5, model order 12 was used. Note that the condition number is equal for the Hessian and the inverse of the Hessian. It can be observed that Method 1 is numerically the most well conditioned method. Method 2 also indicates good numerical behavior, while Method 4 shows a large condition number. A large model order may cause numerical problems for Methods 3–5, cf Section 5.6 and the fact that Method 4 gives comparably many rejections for large model orders in the noise free case (Table 7). However, a smaller condition number results for Method 4 when a smaller model order is used.

Studying the estimated Hessians for the different methods, reflects the fact that the variance of the estimates of C is expected to be larger than that of R. As an example, study Method 1 and Method 3 using $n = 50$ and $n = 12$, respectively.

Method	$\frac{\partial^2 V}{\partial R^2}$	$\frac{\partial^2 V}{\partial C^2}$	$\frac{\partial^2 V}{\partial R \partial C}$	Condition number
1	0.201	0.080	-0.051	3.58
2	275	104	-154	26.5
3	1.30	0.013	-0.028	109
4	2.00	3.99×10^{-5}	6.06×10^{-5}	5.01×10^{4}
5	65.9	0.681	-1.52	102

Table 8: The Hessians for different methods and their condition numbers.

Here the inverse of the Hessians are given by, cf (76),

$$\left(V_1''(\theta)\right)^{-1} = \begin{pmatrix} 5.94 & 3.78 \\ 3.78 & 14.91 \end{pmatrix} \tag{79}$$

$$\left(V_3''(\theta)\right)^{-1} = \begin{pmatrix} 0.807 & 1.74 \\ 1.74 & 80.67 \end{pmatrix} \tag{80}$$

It can be noted that the $(2,2)$ elements of (79)–(80) are larger than the $(1,1)$ elements. Therefore the bias as well as the variance of $\hat{C}$ is expected to be greater than that of $\hat{R}$, according to the discussion above.

5.7.2 Identification from noise-corrupted data

In this test, the system output, T_i, contains additional noise. The noise level is 15 dB below the average level of T_i, cf Figure 10. The noise is white, while the signal is of low pass character. Therefore, the noise affects the higher frequencies more. Tables 9–10 display the estimated parameters in the case of noisy output signal, T_i. (No prefiltering of signals was performed when obtaining the results in the tables).

It is clear that presence of stochastic measurement noise results in parameter estimates with a stochastic errors. Especially Methods 3–5 seem to be sensitive to additive noise. There is hence a need for decreasing the influence of the disturbance. Filtering of the signals is a commonly used way of reducing the relative amount of noise. Since the data are of low pass character (slow variations of the temperature) and since it is known that the transfer functions to be estimated are of low pass character too, it is appropriate to emphasize the lower frequencies.

A simple Butterworth filter of second order with the cut-off frequency 1/(12h), corresponding to half the signal period, was applied to the signals involved in the identification procedure. The results are shown in Tables 11–12. The same data series were used here as was used in the case when no filtering was involved.

In Figures 21 and 22, the bias and standard deviation of estimates of Method 1 and Method 3 are presented, as a complement to the tables.

For all methods, a considerable improvement of identification results was obtained when the signals were low-pass filtered prior to identification. Especially, advantage of filtering could be shown for Methods 3–5.

Model order n	Results from Methods 1–2 1	2	Rejections 1	2
10	$\hat{R} = 7.80$	$\hat{R} = 9.45$	–	–
	$\hat{C} = 17.82$	$\hat{C} = 22.47$	–	–
15	$\hat{R} = 8.62$	$\hat{R} = 9.89$	–	–
	$\hat{C} = 17.08$	$\hat{C} = 19.99$	–	–
20	$\hat{R} = 9.05$	$\hat{R} = 9.84$	–	–
	$\hat{C} = 16.59$	$\hat{C} = 18.47$	–	–
30	$\hat{R} = 9.45$	$\hat{R} = 9.94$	–	–
	$\hat{C} = 16.09$	$\hat{C} = 17.04$	–	–
40	$\hat{R} = 9.63$	$\hat{R} = 9.91$	–	–
	$\hat{C} = 15.81$	$\hat{C} = 16.35$	–	–
50	$\hat{R} = 9.73$	$\hat{R} = 9.93$	–	–
	$\hat{C} = 15.63$	$\hat{C} = 17.02$	–	–
∞	$\hat{R} = 10.01$	$\hat{R} = 9.90$	–	–
	$\hat{C} = 15.04$	$\hat{C} = 14.88$	–	–

Table 9: Result of parameter estimation for Methods 1–2, with noise on the output signal and no prefiltering. In the true system, R equals 10 $[^oCm^2/W]$ and C equals 15 $[Wh/^oCm^2]$.

Model order n	Results from Methods 3–5 3	4	5	Rejections 3	4	5
4	$\hat{R} = 4.66$	$\hat{R} = 4.66$	$\hat{R} = 4.66$	–	–	–
	$\hat{C} = 6.27$	$\hat{C} = 3.78$	$\hat{C} = 8.58$	–	–	–
6	$\hat{R} = 6.48$	$\hat{R} = 6.48$	$\hat{R} = 6.49$	–	–	–
	$\hat{C} = 7.69$	$\hat{C} = 4.64$	$\hat{C} = 9.62$	–	–	–
8	$\hat{R} = 7.74$	$\hat{R} = 7.74$	$\hat{R} = 7.74$	–	–	–
	$\hat{C} = 8.86$	$\hat{C} = 5.22$	$\hat{C} = 10.54$	–	–	–
10	$\hat{R} = 8.48$	$\hat{R} = 8.47$	$\hat{R} = 8.48$	–	–	–
	$\hat{C} = 9.92$	$\hat{C} = 6.09$	$\hat{C} = 11.43$	–	–	–
11	$\hat{R} = 8.81$	$\hat{R} = 8.60$	$\hat{R} = 8.61$	–	–	–
	$\hat{C} = 10.55$	$\hat{C} = 7.03$	$\hat{C} = 12.01$	–	–	–
12	$\hat{R} = 8.99$	$\hat{R} = 8.98$	$\hat{R} = 8.99$	–	–	–
	$\hat{C} = 10.97$	$\hat{C} = 7.22$	$\hat{C} = 12.37$	–	–	–

Table 10: Result of parameter estimation for Methods 3–5, with noise on the output signal and no prefiltering. In the true system, R equals 10 $[^oCm^2/W]$ and C equals 15 $[Wh/^oCm^2]$.

Model order n	Results from Methods 1–2 1	2	Rejections 1	2
10	$\hat{R} = 8.63$	$\hat{R} = 9.71$	–	–
	$\hat{C} = 17.95$	$\hat{C} = 19.31$	–	–
15	$\hat{R} = 9.16$	$\hat{R} = 9.90$	–	–
	$\hat{C} = 17.03$	$\hat{C} = 17.85$	–	–
20	$\hat{R} = 9.41$	$\hat{R} = 9.93$	–	–
	$\hat{C} = 16.55$	$\hat{C} = 17.03$	–	–
30	$\hat{R} = 9.63$	$\hat{R} = 9.93$	–	–
	$\hat{C} = 16.03$	$\hat{C} = 16.22$	–	–
40	$\hat{R} = 9.73$	$\hat{R} = 9.92$	–	–
	$\hat{C} = 15.76$	$\hat{C} = 15.82$	–	–
50	$\hat{R} = 9.78$	$\hat{R} = 9.93$	–	–
	$\hat{C} = 15.60$	$\hat{C} = 16.22$	–	–
∞	$\hat{R} = 10.03$	$\hat{R} = 9.91$	–	–
	$\hat{C} = 15.03$	$\hat{C} = 14.82$	–	–

Table 11: Result of parameter estimation for Methods 1–2, with noise on the output signal. The data has been filtered through a low pass filter prior to the parameter estimation. In the true system, R equals 10 $[^oCm^2/W]$ and C equals 15 $[Wh/^oCm^2]$.

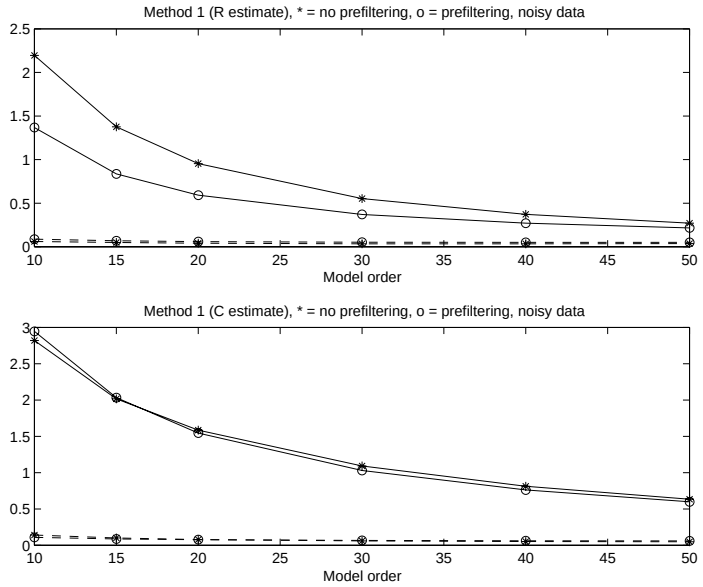

Figure 21: Bias (solid lines) and standard deviation (dashed lines) of $\hat{R}$ and $\hat{C}$ obtained from Method 1 for noisy data. Lines with stars ($*$) indicate no prefiltering and circles (o) indicate prefiltering of data.

Model order	Results from Methods 3–5			Rejection		
n	3	4	5	3	4	5
4	$\hat{R} = 10.44$	$\hat{R} = 10.44$	$\hat{R} = 10.42$	–	–	–
	$\hat{C} = 14.69$	$\hat{C} = 13.07$	$\hat{C} = 20.49$	–	–	–
6	$\hat{R} = 10.39$	$\hat{R} = 10.39$	$\hat{R} = 10.39$	–	–	–
	$\hat{C} = 14.26$	$\hat{C} = 12.60$	$\hat{C} = 18.06$	–	–	–
8	$\hat{R} = 10.38$	$\hat{R} = 10.37$	$\hat{R} = 10.38$	–	–	–
	$\hat{C} = 14.29$	$\hat{C} = 12.59$	$\hat{C} = 17.14$	–	–	–
10	$\hat{R} = 10.35$	$\hat{R} = 10.35$	$\hat{R} = 10.36$	–	–	–
	$\hat{C} = 14.34$	$\hat{C} = 12.71$	$\hat{C} = 16.62$	–	–	–
11	$\hat{R} = 10.11$	$\hat{R} = 10.20$	$\hat{R} = 10.20$	–	–	–
	$\hat{C} = 13.36$	$\hat{C} = 12.01$	$\hat{C} = 16.10$	–	–	–
12	$\hat{R} = 10.36$	$\hat{R} = 10.36$	$\hat{R} = 10.36$	–	–	–
	$\hat{C} = 14.47$	$\hat{C} = 13.01$	$\hat{C} = 16.39$	–	–	–

Table 12: Result of parameter estimation for Methods 3–5, with noise on the output signal. The data has been filtered through a low pass filter prior to the parameter estimation. In the true system, R equals 10 $[^oCm^2/W]$ and C equals 15 $[Wh/^oCm^2]$

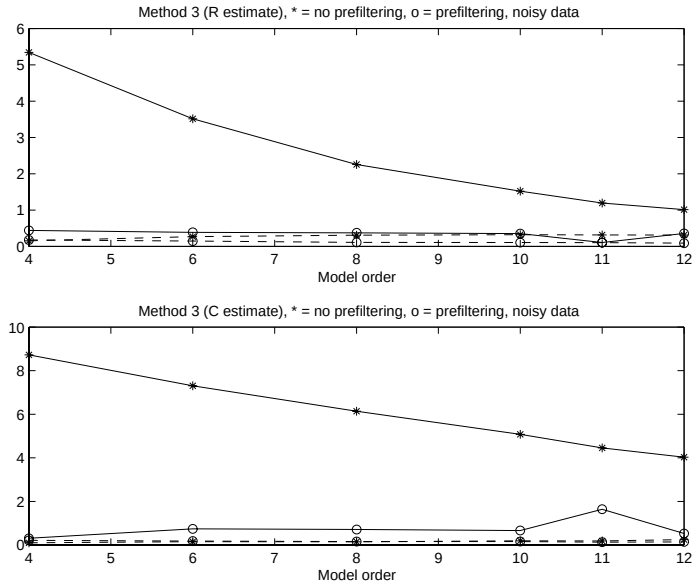

Figure 22: Bias (solid lines) and standard deviation (dashed lines) of $\hat{R}$ and $\hat{C}$ obtained from Method 3 for noisy data. Lines with stars ($*$) indicate no prefiltering and circles (o) indicate prefiltering of data.

6 Conclusions

Five methods for parameter estimation of diffusion models have been presented. The methods derived in the paper can essentially be divided into two groups; direct approaches and indirect approaches cf Sections 4.1–4.3. The methods in the two groups have similar behavior. In the direct approaches (Methods 1–2), a model output is fitted to the given output measurement. In the indirect approaches (Methods 3–5), the transfer function of the system is first estimated using some standard black-box technique. In a second step the system parameters are then extracted from the estimated transfer function. Of particular concern in the study is the effects of approximating the dynamics, which is of infinite order, by a finite-order model.

Several conclusions can be drawn from the evaluations. A model of large order describes the system dynamics well, and hence improves the estimates, but some drawbacks may occur. Using large model orders results in increasing computational load, especially for Methods 1 and 2. If complexity is not considered as a problem, a large model order may be used for the direct approaches since the estimation errors due to a finite order model decreases. For the indirect approaches, however, utilizing a black-box model, numerical problems might occur for larger model orders, resulting in bad parameter estimates. This is a serious problem, but can be avoided through the use of a scheme for model validation, see Section 5.6.

It can also be observed that the direct approaches require larger model orders than the indirect approaches in order to obtain approximately equal accuracy on the estimates.

The indirect approaches are more sensitive to noise on the output than the direct approaches. The indirect approaches give, however, even for noisy data, a bias of only a few percent when the data are prefiltered with a low pass filter prior to the parameter estimation.

References

[1] H. T. Banks and K. Kunich. *Estimation Techniques for Distributed Parameter Systems.* Birkhäuser, Boston, 1989.

[2] A. Tarantola. *Inverse Problem Theory.* Elsevier, 1987.

[3] K. Kunisch. Numerical methods for parameter estimation problems. In *Inverse Problems in Diffusion Processes.* SIAM, 1995.

[4] T. Söderström and P. Stoica. *System Identification.* Prentice Hall International, Hemel Hemstead, 1989.

[5] L. Ljung. *System Identification – Theory for the User.* Prentice-Hall, Englewood Cliffs, 1987.

[6] T. Bohlin and S. F. Graebe. Issues in nonlinear stochastic grey box identification. *International Journal of Adaptive Control and Signal Processing*, 9(6):465–490, 1995.

[7] G. Chavent. Identification of distributed parameter systems: about the output least square method, its implementation, and identifiability. In *Proc. 5th IFAC Symposium on Identification and System Parameter Estimation*, 1979.

[8] C. S. Kubrusly. Distributed parameter system identification – a survey. *International Journal of Control*, 26(4):509–535, 1977.

[9] M. P. Polis. The distributed system parameter identification problem: a survey of recent results. In *Proc. 3rd IFAC Conf on Control of Distributed Parameter Systems*, 1982.

[10] P. Stoica T. Söderström and B. Friedlander. An indirect prediction error method for system identification. *Automatica*, 27(1):183–188, 1991.

[11] B. Wahlberg and L. Ljung. Design variables for bias distribution in transfer function estimates. *IEEE Trans. Automatic Control*, AC-31(2):134–144, 1986.

[12] G. H. Golub and J. M. Ortega. *Scientific Computing and Differential Equations.* Academic Press, San Diego, 1981.